

US EPA ARCHIVE DOCUMENT



Three-Dimensional Numerical Modeling of Morrow Lake in Kalamazoo River, Michigan

Zhenduo Zhu¹
Marcelo H. Garcia²

¹Graduate Research Assistant

²Professor and Director

Ven Te Chow Hydrosystems Laboratory

Prepared for:

**U.S. Environmental Protection Agency
Region 5
Chicago, IL 60604-3590**



Ven Te Chow Hydrosystems Laboratory
Civil and Environmental Engineering
University of Illinois
Urbana, Illinois

July 2015

**Three-Dimensional Numerical Modeling of Morrow Lake
in Kalamazoo River, Michigan**

by

Zhenduo Zhu and Marcelo H. García

Ven Te Chow Hydrosystems Laboratory

Department of Civil and Environmental Engineering

University of Illinois at Urbana and Champaign, IL



Table of Contents

Executive Summary	6
1. Introduction.....	7
1.1 Study Domain	7
2. Description of the Numerical Model	9
2.1 Computational Meshes.....	9
2.2 Bathymetry.....	10
2.3 Model Simulation Scenarios	11
2.4 Boundary Conditions	11
2.5 Other Data Used.....	17
2.5.1 Stage Recorder Data	17
2.5.2 ADCP Survey Data	17
3. Model Results and Discussion.....	19
3.1 Model Calibration	19
3.2 Model Validation.....	20
3.3 Hydrodynamics Analysis	23
3.3.1 Effect of Wind.....	23
3.3.2 Effect of Inflow Flux on Bed Shear Stress Distribution.....	24
3.3.3 Effect of Dam Operation.....	25
3.3.4 Sectional View of Velocity Distribution (Q = 3060 cfs).....	26
3.4 OPA Tracking Model Results.....	27
3.4.1 April 2013 High Flow Scenario	28
3.4.2 July 2013 Low Flow Scenario	34
4. Model Applications.....	36
4.1 Containment Scenario.....	36
4.2 Lake Drawdown Scenario.....	43
5. Summary.....	46
Acknowledgments.....	47
Bibliography	48

Table of Figures

Figure 1. Study Domain and USGS Stations' Location	7
Figure 2. Upstream Boundary at MP 36.5	8
Figure 3. Plan View of the Computational Meshes	9
Figure 4. Sectional View of Computational Meshes at Three Cross Sections.....	10
Figure 5. Bed Elevation of Morrow Lake and Delta (NAVD88)	10
Figure 6. Historical Flow Record at USGS Comstock Station.....	11
Figure 7. Discharge of April 2013 High Flow Scenario Measured at USGS Gauging Stations... 12	
Figure 8. Structures at the Morrow Dam.....	13
Figure 9. Comparison of Measured Outflow Discharge at Kalamazoo River at Comstock and Measured Lake Level at Upstream of Morrow Dam.....	14
Figure 10. Sectional View of Grids Representing Morrow Dam	15
Figure 11. Outflow Distribution at Morrow Dam during April 2013 High Flows	16
Figure 12. Upstream Stage Level of April 2013 High Flow Scenario at MP 36.5	16
Figure 13. Location of Kalamazoo/Battle Creek Intl. Airport (wind data)	16
Figure 14. Locations of Stage Recorder at Morrow Lake and Delta.....	17
Figure 15. ADCP Transects Measurement Locations.....	18
Figure 16. ADCP Stationary Measurement Locations	18
Figure 17. Roughness Height Calibration with April 2013 High Flow Scenario	19
Figure 18. Model Validation with Stage Level in July 2013 Low Flow Scenario.....	21
Figure 19. Comparison of Bed Shear Stress and Depth-Averaged Velocity between Stationary ADCP Measurement (x-axis) and Simulation Results (y-axis).....	22
Figure 20. An Example of ADCP Data Processing	22
Figure 21. Sectional View of Velocity Distribution at MP 38.5 (with wind)	23
Figure 22. Sectional View of Velocity Distribution at MP 38.5 (without wind)	23
Figure 23. Bed Shear Stress Distribution at Discharge $Q = 3790$ cfs.....	24
Figure 24. Bed Shear Stress Distribution at Discharge $Q = 434$ cfs.....	24
Figure 25. Velocity and Bed Shear Stress Distribution near Morrow Dam ($Q = 868$ cfs, three turbines in operation).....	25
Figure 26. Velocity and Bed Shear Stress Distribution near Morrow Dam ($Q = 1950$ cfs, four turbines and flap gate in operation)	25
Figure 27. Velocity and Bed Shear Stress Distribution near Morrow Dam ($Q = 3650$ cfs, four turbines, flap gate, and tainter gate in operation)	26
Figure 28. Plan and Sectional View of Velocity Distribution ($Q = 3060$ cfs)	27
Figure 29. OPA Particle Locations at Time = 0 hour.....	28

Figure 30. OPA Particle Locations at Time = 4 hour (Q = 690 cfs)	29
Figure 31. OPA Particle Locations at Time = 24 hour (Q = 868 cfs)	29
Figure 32. OPA Particle Locations at Time = 2 day (Q = 884 cfs).....	30
Figure 33. OPA Particle Locations at Time = 4 day (Q = 1940 cfs).....	30
Figure 34. OPA Particle Locations at Time = 8 day (Q = 2440 cfs).....	31
Figure 35. OPA Particle Locations at Time = 13 day (Q = 3660 cfs).....	31
Figure 36. OPA Particle Locations at Time = 15 day (Q = 3230 cfs).....	32
Figure 37. OPA Particle Locations at Time = 20 day (Q = 2250 cfs).....	32
Figure 38. Types of OPA	33
Figure 39. OPA Particle Locations at the end of simulation.....	33
Figure 40. OPA Particle (Type 1) Locations at Time = 10 day (July 2013 Scenario)	34
Figure 41. OPA Particle (Type 2) Locations at Time = 10 day (July 2013 Scenario)	34
Figure 42. OPA Particle (Type 3) Locations at Time = 10 day (July 2013 Scenario)	35
Figure 43. OPA Particle Locations at Time = 10 day (July 2013 Scenario with lighter particles).....	35
Figure 44. Location of Containment and Representative EFDC Grids	37
Figure 45. Curtain Vertical Detail.....	37
Figure 46. Containment Plan View.....	37
Figure 47. A Side View of Vertical Profile of EFDC Grids Representing Bottom Curtain.....	38
Figure 48. Data of Dam Outflow Discharge (green line) and Stage Level (scatter with green line)	39
Figure 49. Cross-sections for Flow Discharge Check	39
Figure 50. Deposition (black ellipse) and Erosion (purple ellipse) Areas with Velocity Difference between the scenarios with and without Containment	40
Figure 51. Location of Containment C1 and D	41
Figure 52. Distribution of Bed Shear Stress (with Original Containment Design).....	42
Figure 53. Distribution of Bed Shear Stress (without Containment D and Half C1).....	42
Figure 54. Distribution of Bed Shear Stress (without Containment C1).....	42
Figure 55. Distribution of Bed Shear Stress (Q = 585 cfs; DS Level = 775 ft).....	43
Figure 56. Distribution of Bed Shear Stress (Q = 585 cfs; DS Level = 773 ft).....	43
Figure 57. Distribution of Bed Shear Stress (Q = 585 cfs; DS Level = 771 ft).....	44
Figure 58. Distribution of Bed Shear Stress (Q = 794 cfs; DS Level = 775 ft).....	44
Figure 59. Distribution of Bed Shear Stress (Q = 794 cfs; DS Level = 773 ft).....	44

Executive Summary

The July 2010 spill of diluted bitumen into the Kalamazoo River was the largest release of heavy crude into an inland waterway in U.S. history. Since the spill, extensive cleanup and recovery efforts have taken place. However, substantial residual deposits from the oil spill remained in the river system due to formation of oil-particle aggregates (OPA) and their negative buoyancy. It is important to understand the conditions under which OPA can be re-suspended, transported and re-deposited. Once OPA pass through Morrow Lake, they have the potential to continue to migrate all the way toward Lake Michigan.

A three-dimensional model for OPA transport and fate in Morrow Lake and its delta was built with the Environmental Fluid Dynamics Code (EFDC). The three-dimensional model enabled consideration of hydrodynamic effects of inflow fluxes on OPA movements through the delta and neck areas before entering Morrow Lake, the Morrow Lake dam operational rules as well as wind effects, which might increase the risk of resuspension and transport of OPA downstream into the Kalamazoo River. A Lagrangian particle tracking model was developed and coupled with the hydrodynamics model with the objective of simulating the transport and fate of OPA.

The April 2013 high flow scenario and the July 2013 low flow scenario were modeled. The model was calibrated and validated using field measurement data. The model was also applied to two scenarios, evaluating the effects of containment layouts and lake drawdown for excavation, which demonstrated the utility of the numerical model in assisting with management decisions for cleanup and restoration.

1. Introduction

Following the oil spill at Kalamazoo River waterways system in 2010, extensive oil cleanup and environmental remediation efforts have taken place. Because of recurrences of oil sheen and other problems, one of the biggest concerns was to understand the conditions under which the remaining submerged oil particle aggregates (OPA) became re-suspended, transported and re-deposited. A three-dimensional hydrodynamics model coupled with a three-dimensional Lagrangian particle tracking model was implemented to model the movement of OPA in Morrow Lake and its delta. It was hoped that the model simulation could practically predict the depositional areas of OPA and help with lake management to prevent oil and OPA from migrating toward Lake Michigan.

1.1 Study Domain

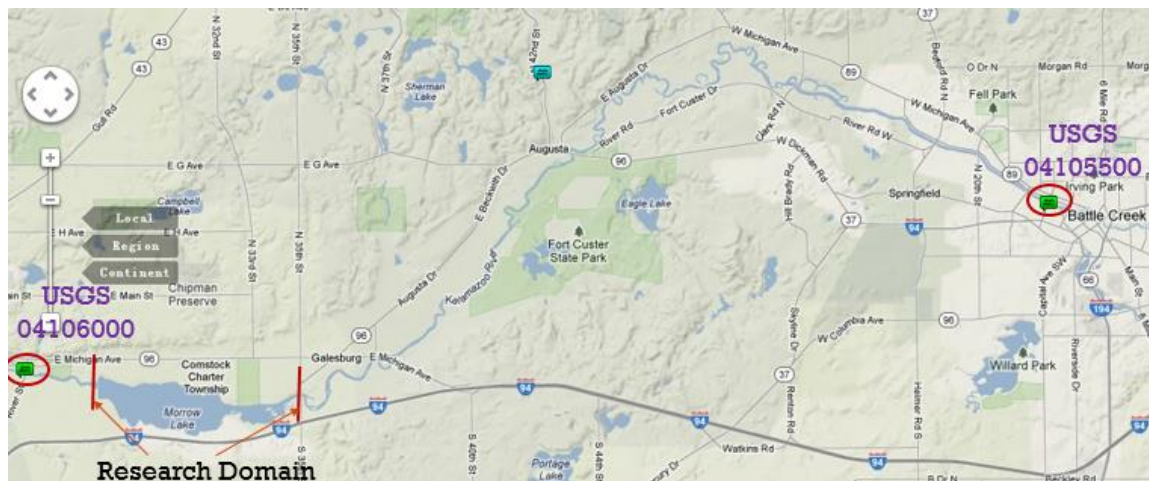


Figure 1. Study Domain and USGS Stations' Location
(Image from <http://www.wunderground.com/wundermap/>)

Figure 1 shows the upstream and downstream boundaries of the study reach. The numerical model focused on the domain of Morrow Lake and its delta (Figure 2). The upstream boundary was at Mile Post (MP) 36.5 (see Figure 2), while the downstream boundary was at the Morrow Dam, which contains structures for controlling outflows of the lake for power generation, recreation, flood control, and other purposes. The domain was approximately 3.5 miles long. By different operation of Morrow Dam, the stage

level of Morrow Lake can be modified higher or lower due to the difference between inflow and outflow.



Figure 2. Upstream Boundary at MP 36.5

2. Description of the Numerical Model

Environmental Fluid Dynamics Code (EFDC) was used in this study. EFDC is a public domain code which can model both hydrodynamics and water quality for surface water systems. It was originally developed at the Virginia Institute of Marine Science (Hamrick, 1992) and has been widely used since then for surface water issues involving rivers, lakes, estuaries, coastal regions and wetlands. The Ven Te Chow Hydrosystems Laboratory at the University of Illinois at Urbana-Champaign has applied EFDC to the Chicago River and associated waterways in several projects (Sinha et al. 2012, 2013). Through those projects, the Ven Te Chow Hydrosystems Laboratory modified EFDC for improving the functionalities especially in parallelization, robust coupling with other models and so on. In this study, the authors implemented a three-dimensional Lagrangian particle tracking model into EFDC for the modeling of OPA entrainment, transport and fate.

2.1 Computational Meshes

The Morrow Lake model used curvilinear orthogonal grids, which consisted of 16,206 cells in the (x, y) plane (Figure 3) and 8 vertical layers (Figure 4). The size of the horizontal cells was approximately 60 feet by 60 feet.

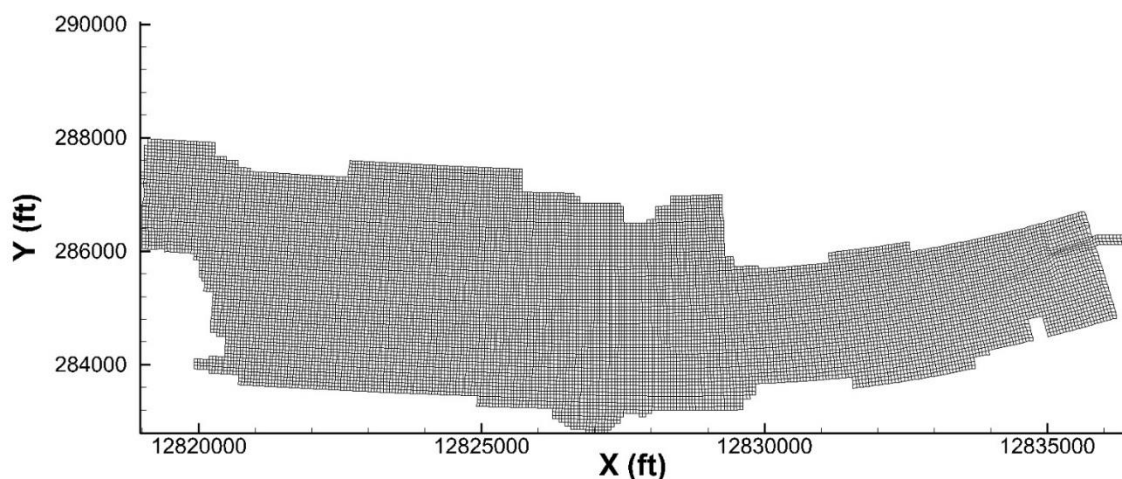


Figure 3. Plan View of the Computational Mesh for Morrow Lake, Michigan

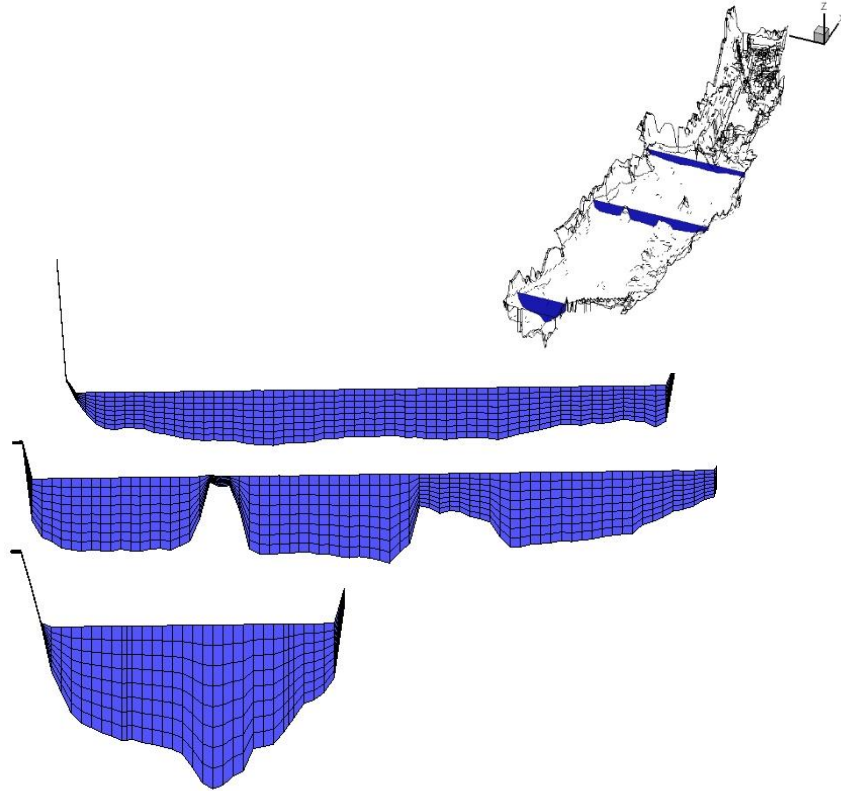


Figure 4. Sectional View of Computational Meshes at Three Cross Sections

2.2 Bathymetry

The bathymetry data was provided by Weston Solutions, Inc. (Weston, 2014/02/19 version). The bed elevation was interpolated to the center of each grid cell with the help of an in-house FORTRAN code.

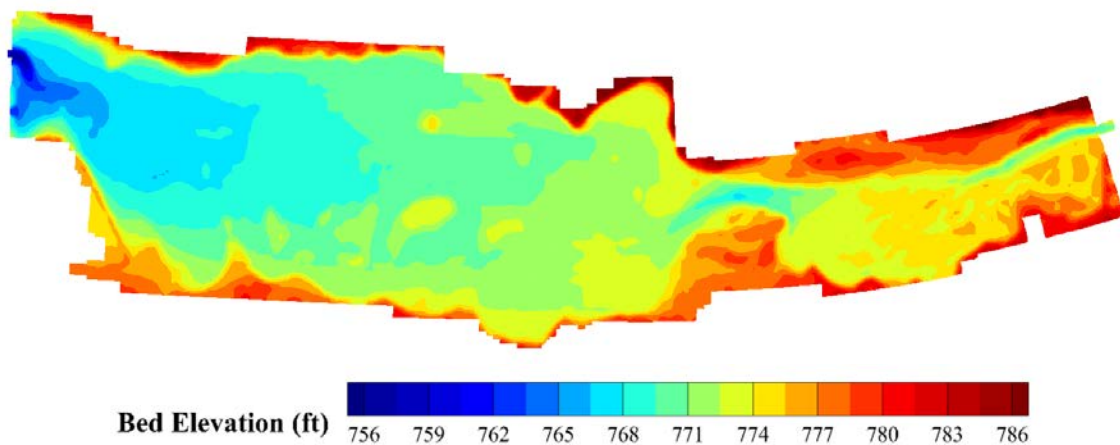


Figure 5. Bed Elevation of Morrow Lake and Delta (NAVD88)

2.3 Model Simulation Scenarios

Two flow scenarios were simulated to represent high inflow and low inflow fluxes, respectively. Figure 6 shows the historical flow record (1933-2013) at the USGS gauging station 04106000, located downstream of Morrow Lake (see Figure 1). The daily mean discharge of April and July 2013 events is shown by blue and red circles, respectively. It indicates that the peak of the April 2013 flow is higher than the 95th percentile of daily mean value for those dates in the last 80 years. A July 2013 flow event is slightly under the median daily mean value in July, one of the lowest flow period within a year. These two flow events (April 9 – 29, 2013 and July 9 - 19, 2013) were selected because of the availability of ADCP and stage recorder data for model calibration and validation.

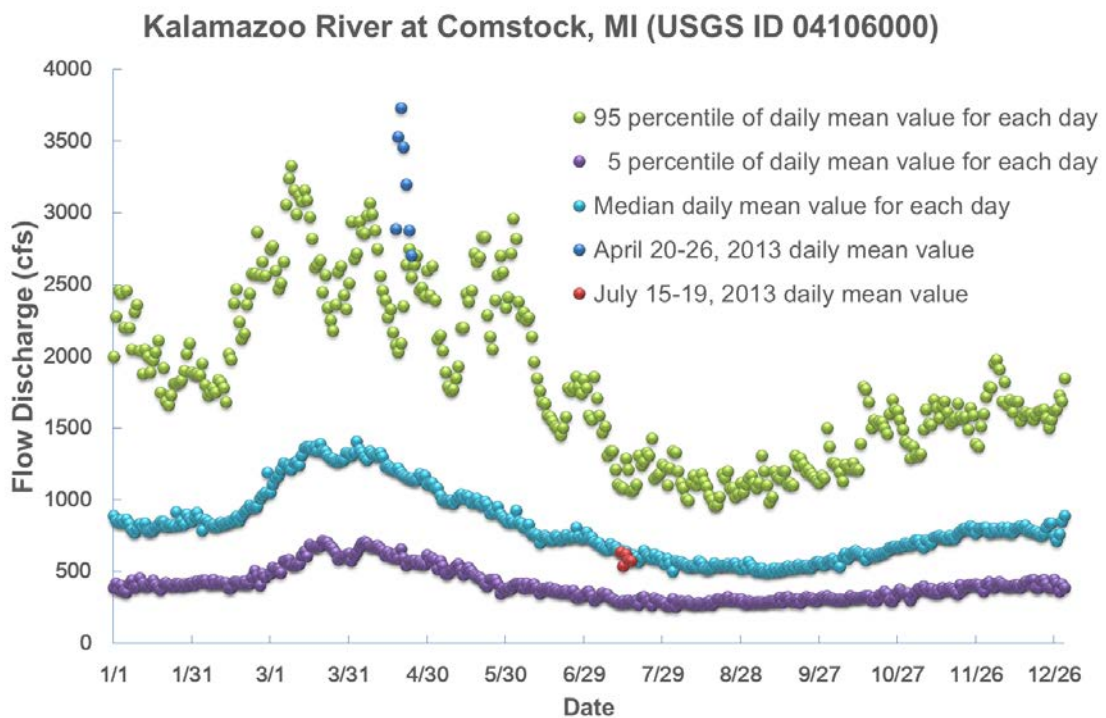


Figure 6. Historical Flow Record at USGS Comstock Station (USGS04106000)

2.4 Boundary Conditions

There exist two USGS gauging stations (see Figure 1) for providing continuous flow discharge measurement to the study reach, one upstream near Battle Creek

(USGS04105500) and the other one downstream at Comstock (USGS04106000). The downstream gauge at Comstock is located roughly 1 mile downstream of Morrow Lake Dam so that it indicates outflow discharge from Morrow Dam. Conversely, there are several tributaries in the reach between the upstream station (near Battle Creek) and the upstream boundary of the numerical domain, MP 36.5. Therefore the flow discharge measured at the upstream station near Battle Creek may differ substantially from the inflow discharge of the study domain. The difference can be clearly seen in Figure 7. In other words, for the model domain the outflow discharge was known quite well while the inflow discharge was not. However, with the installation of a stage level recorder at MP 36.5, as discussed later, the recorded water levels were used as upstream boundary conditions for both April and July 2013 simulation events.

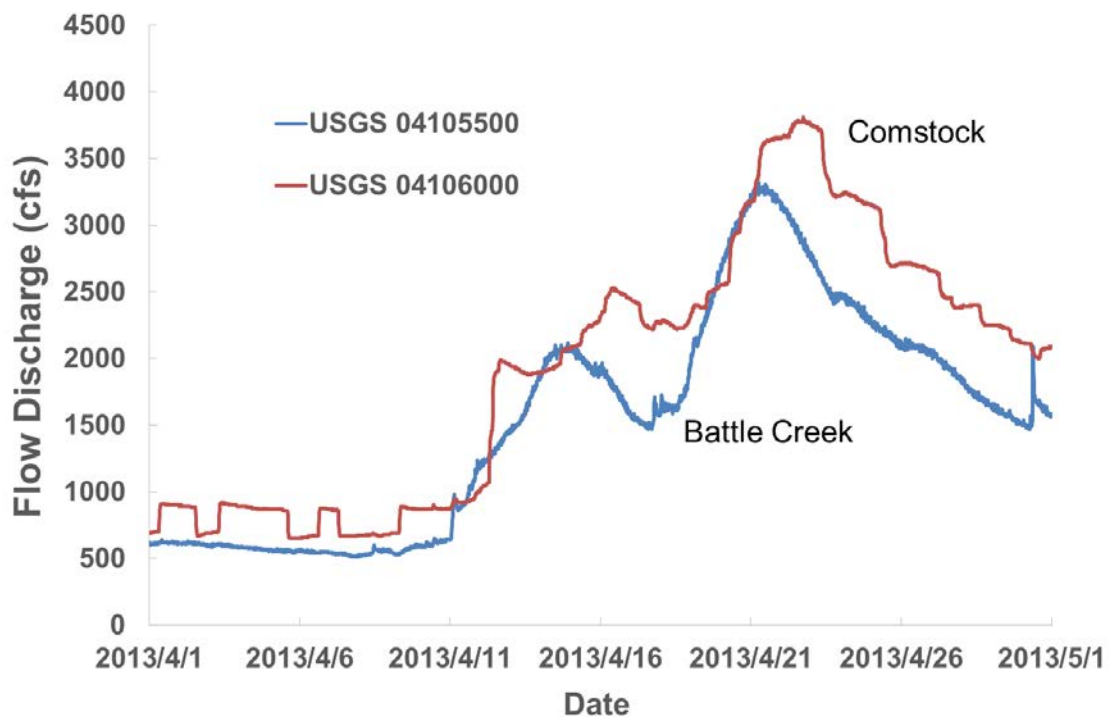


Figure 7. Discharge of April 2013 High Flow Scenario Measured at USGS Gauging Stations

Morrow Dam is owned by a STS Hydropower Ltd (STS) who controls the stage level of Morrow Lake for electricity generation and other purposes. There are two outflow sections at the dam (see Figure 8): one is the powerhouse with four turbines (250 cfs capacity each) and the other section consists of two Tainter gates with flap gates on top of each other. In general, the operator of the dam follows operational rules and an estimated inflow (use USGS gauge station 04105500, Kalamazoo River near Battle

Creek for reference) to maintain the lake level at 776 feet (NGVD). STS recorded lake levels and provided several sets of recorded lake stage to assist with the study. From the comparison of STS stage records and counterpart discharge at Kalamazoo River at Comstock station, it can be expected that from time to time the released discharges deviated from the operational rules. Therefore, although Comstock gauge station provided the outflow discharge, the discharge itself was not sufficient to estimate the stage level solely based on outflow. Figure 9 shows available data of the stage level near the dam against outflow discharge. For a given stage level, the outflow rate can vary all the way from 0 cfs up to 4000 cfs. On the other hand, with a given outflow discharge, stage level can vary up to 1 foot.



Figure 8. Structures at the Morrow Lake Dam

(The glass building to the right (looking upstream) contains the power generators and four turbines underneath. To the left of the glass building are two Tainter gates with flap gates on top.)

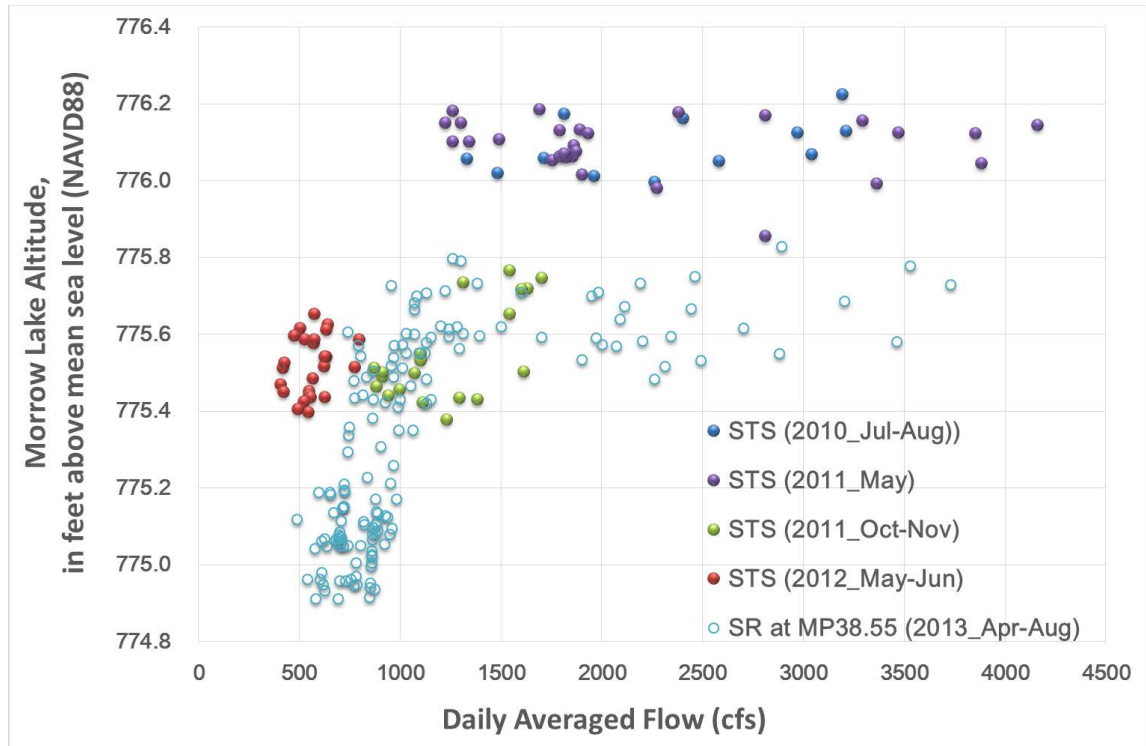


Figure 9. Comparison of Measured Outflow Discharge at Kalamazoo River at Comstock and Measured Lake Level right Upstream of Morrow Dam

For model simulations, it was decided that the most suitable boundary condition to use was the flow discharge downstream of Morrow Dam and the stage level at the upstream (MP 36.5, Figure 12). The effect of operations at Morrow Dam that control the OPA movement was one of the study objectives. Applying the flow boundary condition at the downstream end allowed for the possibility to include dam operation rules. A model can be set up to estimate how much flow passes through turbines, flap gates, and Tainter gates, respectively (Figure 10). The importance of treating each outflow mode independently was that the turbines' inlet was near the bottom while the flap gates' outflow was located at the lake's surface, which yielded different hydrodynamic conditions in the water column. Instead of assuming a vertically uniform outflow distribution throughout the water depth, more accurate hydrodynamics were achieved by specifying outflow through the top or bottom layers under different conditions (see Figure 10). For example, discharging from the top or the bottom would have different effects on the bottom shear stress near the dam. It can be expected that bottom discharge would result in higher bottom shear stresses than those induced by surface discharge.

Discharge from flap gate (overflow) and from Tainter gates (underflow) were computed using rating curve equations provided by the STS operator. In conjunction with reference to the operation rules regarding which control(s) were in operation under a given incoming discharge amount, the discharge time history from the flap gages, Tainter gates, and turbines could be estimated. As an example, the total discharge at Comstock station for the April 2013 event was partitioned (Figure 11) using the technique mentioned above.

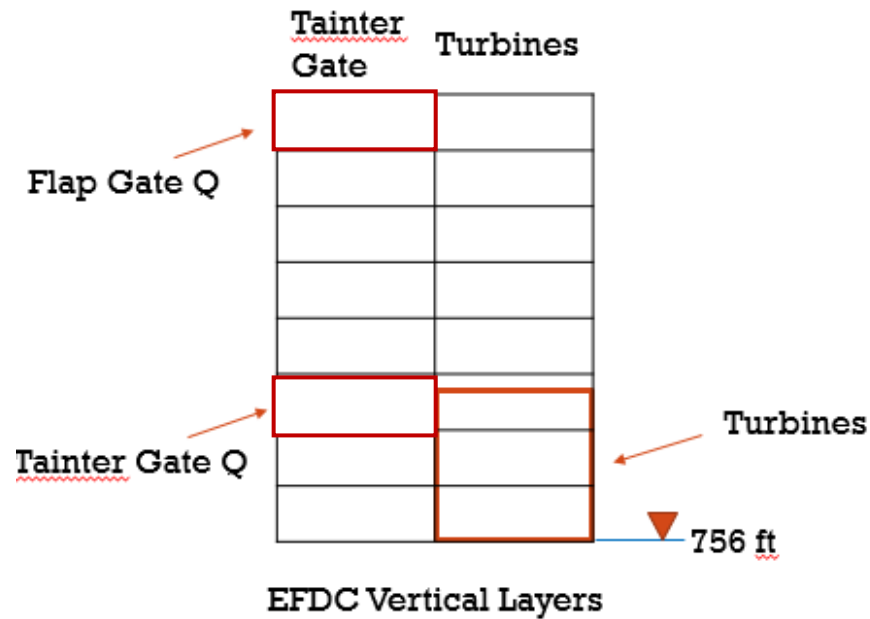


Figure 10. Sectional View of Grids Representing Morrow Dam

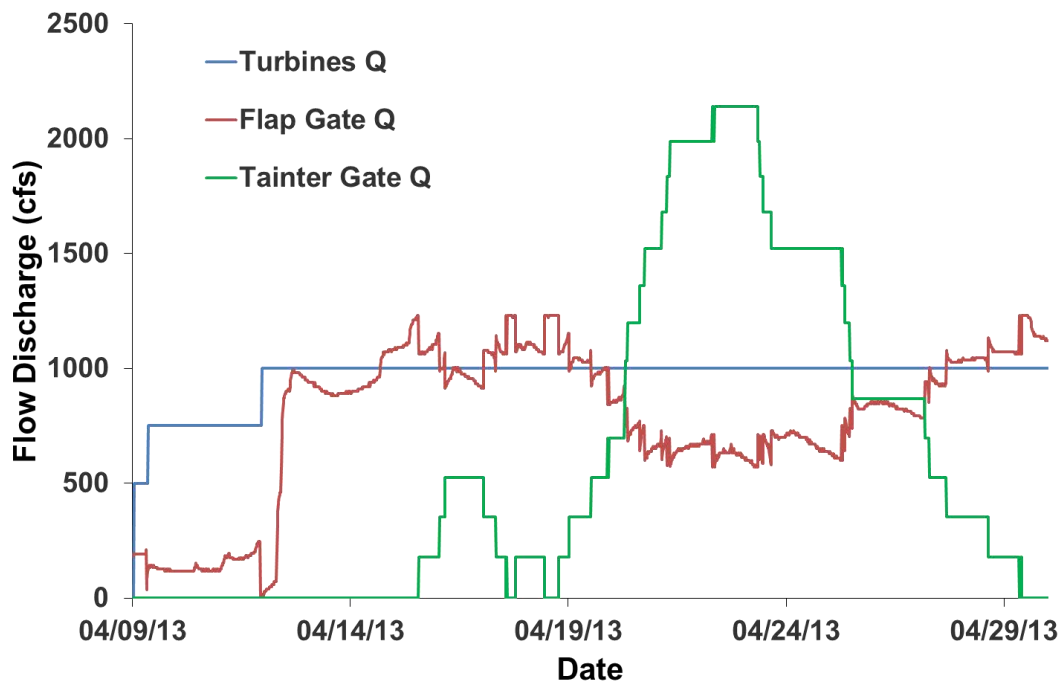


Figure 11. Outflow Distribution at Morrow Dam during April 2013 High Flows

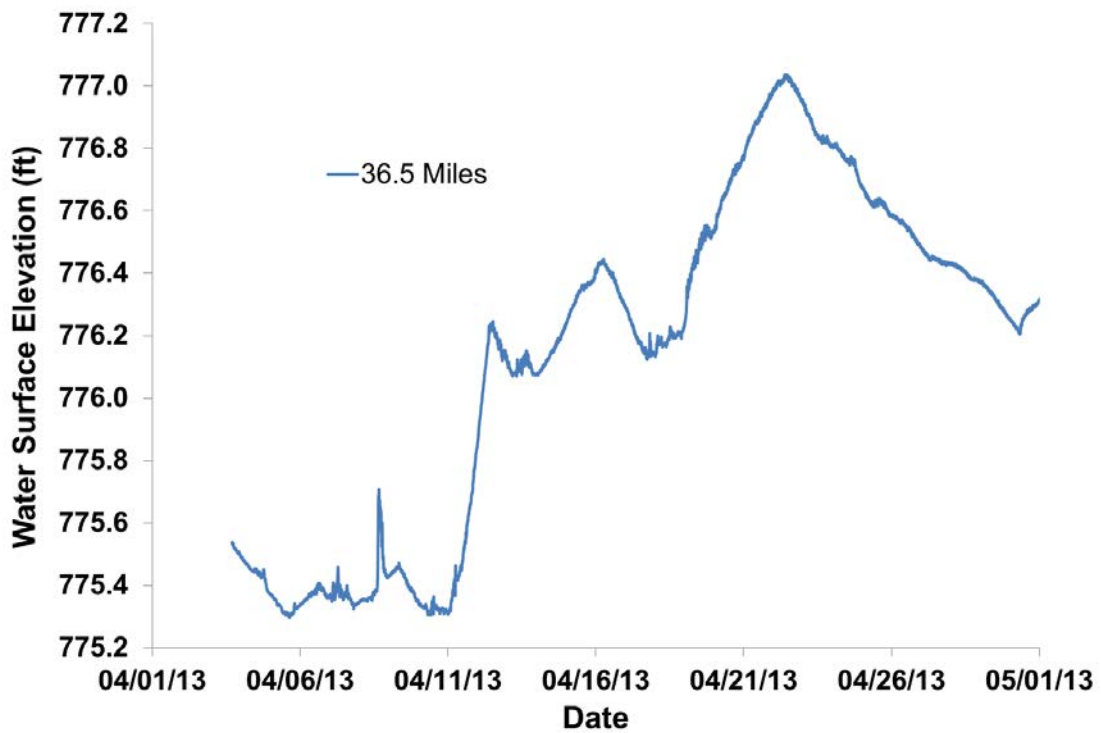


Figure 12. Upstream Stage Level of April 2013 High Flow Scenario at MP 36.5

Wind effects were also considered in the modeling effort. Wind speed and direction data were measured hourly at Kalamazoo/Battle Creek International Airport (see Figure 13), located at approximately 4.4 miles from Morrow Lake (<http://www.ncdc.noaa.gov/cdo-web/>; station 94815).



Figure 13. Location of Kalamazoo/Battle Creek Intl. Airport (wind data)
(Credit: Google Map)

2.5 Other Data Used

Besides USGS gauge station data and stage recorder data at MP 36.5, substantial efforts have been made to collect and analyze other data that are very important for the set-up and calibration of the three-dimensional numerical model.

2.5.1 Stage Recorder Data

Five stage recorders were installed and stage level data were collected from 2013/4/3 to 2013/8/31 (email communication, Paul Reneau, USGS, Wisconsin Water Science Center, 2013/11/11). They were at MP 5.85, MP 14.85, MP 36.50, MP 37.80, and MP 38.55.

Three of them were within the study domain (Figure 14), i.e. MP 36.50, MP 37.80, and MP 38.55 (middle of the lake). As discussed above, the MP 36.5 stage recorder data was used as the upstream boundary condition. The other two were useful for model calibration and validation purposes.



Figure 14. Locations of Stage Recorder at Morrow Lake and Delta

2.5.2 ADCP Survey Data

ADCP surveys were conducted in several periods (email communication, Paul Reneau, USGS Wisconsin Water Science Center, various dates in 2014). The April 2013 survey data was used for comparison with numerical results. There were 47 stationary and 43 transect ADCP measurement from 2013/4/12 to 2013/4/16. In the study domain of Morrow Lake, there were 21 transects and 25 stationary measurements (shown in Figure 15 and Figure 16).



Figure 15. ADCP Transects Measurement Locations



Figure 16. ADCP Stationary Measurement Locations

Stationary ADCP measurement provided vertical velocity profiles. Through analyzing of the vertical profiles, it was possible to estimate the magnitudes of bed shear stress and roughness heights (Reneau et al., 2015). Comparing the derived bed shear stress to those computed by the Morrow Lake EFDC model provided a means for judging the reasonableness of the roughness height parameter used in the numerical model. Bed shear stress is critical in simulating the resuspension or deposition of OPA under the different flow scenarios analyzed in this study.

3. Model Results and Discussion

This chapter summarizes model calibration and validation followed by model results and discussion.

3.1 Model Calibration

Model calibration was accomplished primarily by matching the water surface elevations at selected locations through adjustment of the roughness height at the bed. The comparison of water stage level at MP 38.55 (see Figure 14) between field measurement and numerical results with different bed roughness height is shown in Figure 17. Since floodplain areas were included in the modeling domain, bed roughness height within the floodplain is different from those in riverine and lake areas. Generally it is one order of magnitude higher within the floodplain. Many sets of parameters were tested. Noting that water stage was used as upstream boundary, higher roughness resulted in higher head loss so that water surface elevations would be lower. It was found that the best calibration values were 0.3 mm in lake and riverine areas and 3 mm in floodplain areas.

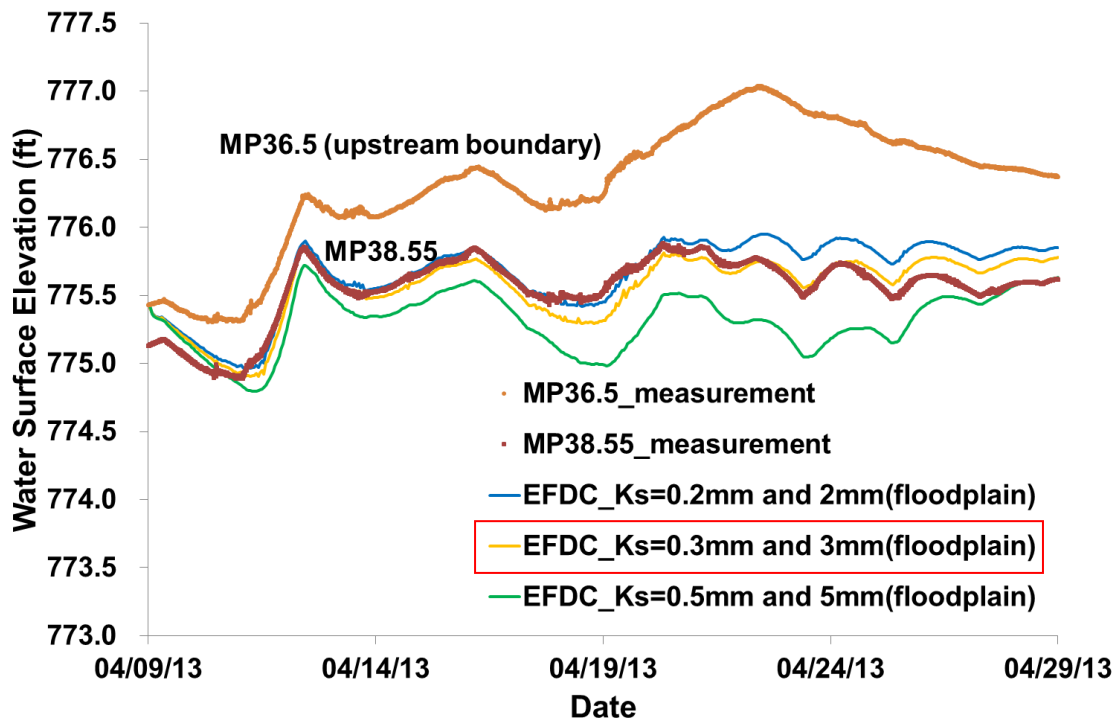


Figure 17. Roughness Height Calibration with April 2013 High Flow Scenario

3.2 Model Validation

Model validation is needed to prove that the model setup and hydrodynamic parameters determined from the calibration flow scenario are also correct for other flow scenarios. The model was validated if it could reproduce the measured water-surface elevations reasonably well at different locations under different flow scenarios.

The July 2013 low flow scenario was used for the validation examination. It was a totally different scenario from the April 2013 high flow scenario (see Figure 6). The peak flow rate during the April 2013 scenario was approximately 3800 cfs; but the flow rate during the July 2013 scenario was in general around 600 cfs and the lowest flow was close to 400 cfs.

Figure 18 shows the comparison of water surface elevations at MP 38.55 between field measurements and model results. Although the model results were generally 0.1 ft higher than the measurement, the difference was acceptable considering the scales and objectives of this study. It is worth mentioning that a better match can surely be achieved if roughness height was adjusted. However in this study, the hydraulics associated with high flow events was the most relevant, and so the same roughness was kept for both April 2013 and July 2013 scenarios.

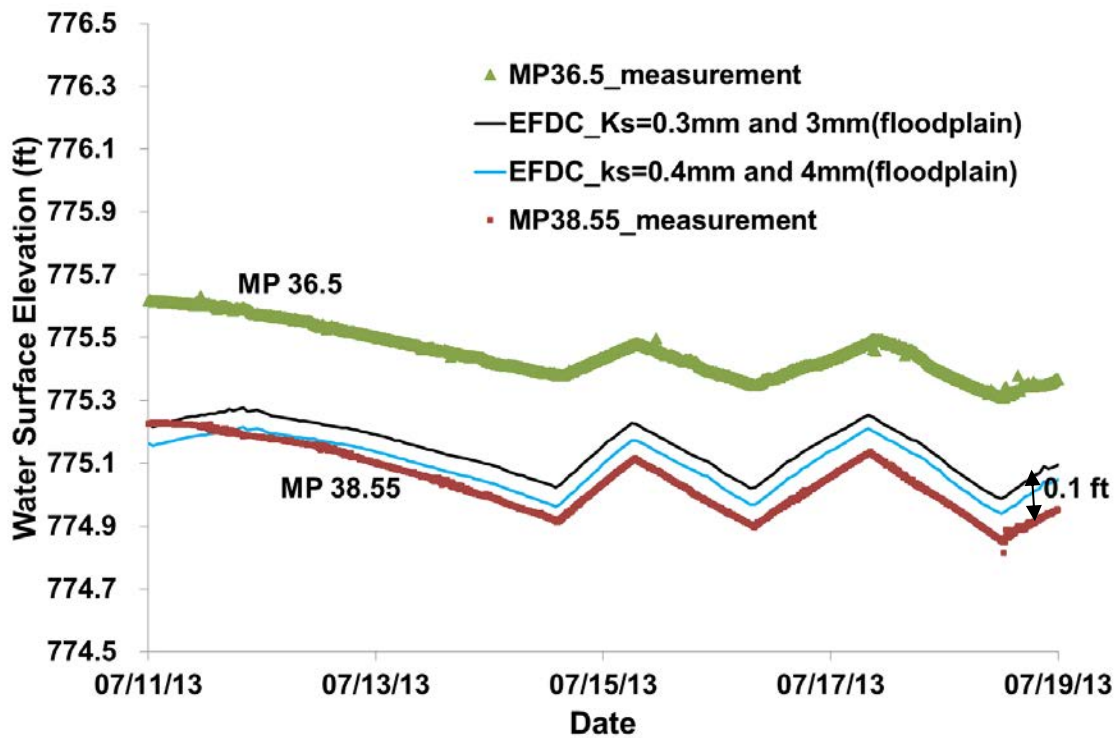


Figure 18. Model Validation with Stage Level in July 2013 Low Flow Scenario

Additional validation was performed using ADCP measurements. Stationary ADCP measurements were used to calculate bed shear stresses by fitting the data to the log law to calculate the shear velocity, which was then converted to the bed shear stress (Reneau, et al., 2015). Comparison with model results is shown in Figure 19. The depth-averaged velocity was also found to give good agreement between model and measurement. An example of ADCP data processing is shown in Figure 20.

The model results of bed shear stress matched quite well with ADCP measurement when they were higher than 0.01 Pa. At very low velocity areas when bed shear stresses were lower than 0.01 Pa, ADCP measurements yielded higher bed shear stress than model results. However, the critical bed shear stress for deposition and resuspension was found to be in the order of 0.1 Pa (Waterman, Fytanidis and Garcia, 2015) so that the difference between model and measurement should not affect the transport of particles too much.

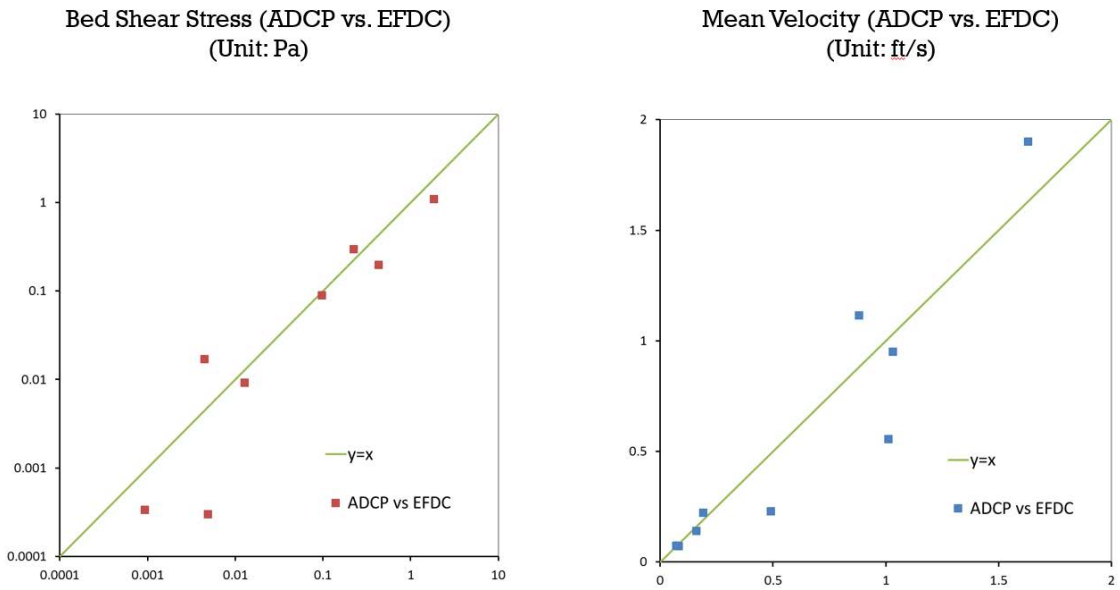


Figure 19. Comparison of Bed Shear Stress and Depth-Averaged Velocity between Stationary ADCP Measurement (x-axis) and Simulation Results (y-axis)

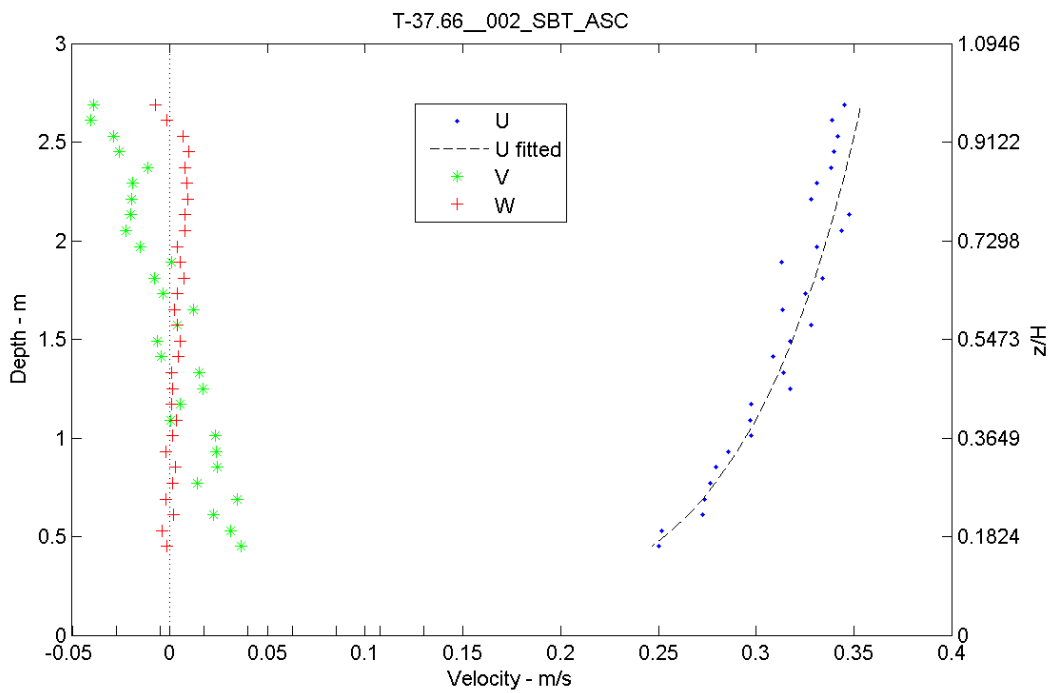


Figure 20. An Example of ADCP Data Processing

3.3 Hydrodynamics Analysis

In this section the effects of wind, inflow flux, and dam operations on hydrodynamics of the lake are discussed.

3.3.1 Effect of Wind

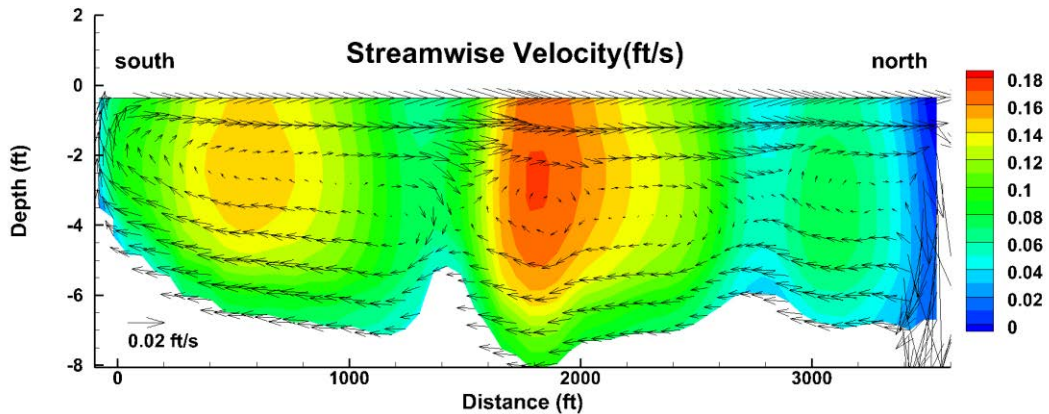


Figure 21. Sectional View of Velocity Distribution at MP 38.5 (with wind)

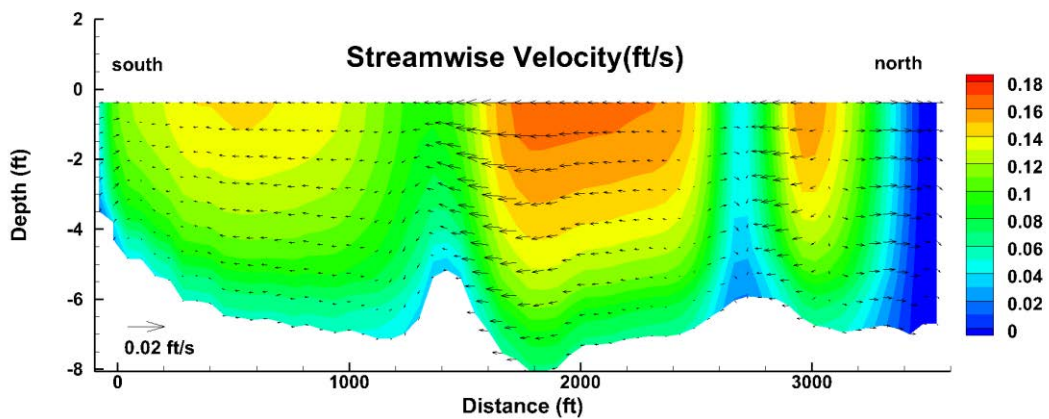


Figure 22. Sectional View of Velocity Distribution at MP 38.5 (without wind)

Figure 21 and Figure 22 compares velocity distribution at the cross section of MP 38.5 with and without wind effect. Note that the colors represent the magnitude of velocity (looking downstream); the vectors represent velocities in the transverse plane. The results were exported at 4/15/2013 18:00 when the wind speed was 6 miles per hour and direction was south to north (i.e. left to right in the sectional view). Wind obviously changed the flow pattern and enhanced the secondary flow depending on wind direction.

3.3.2 Effect of Inflow Flux on Bed Shear Stress Distribution

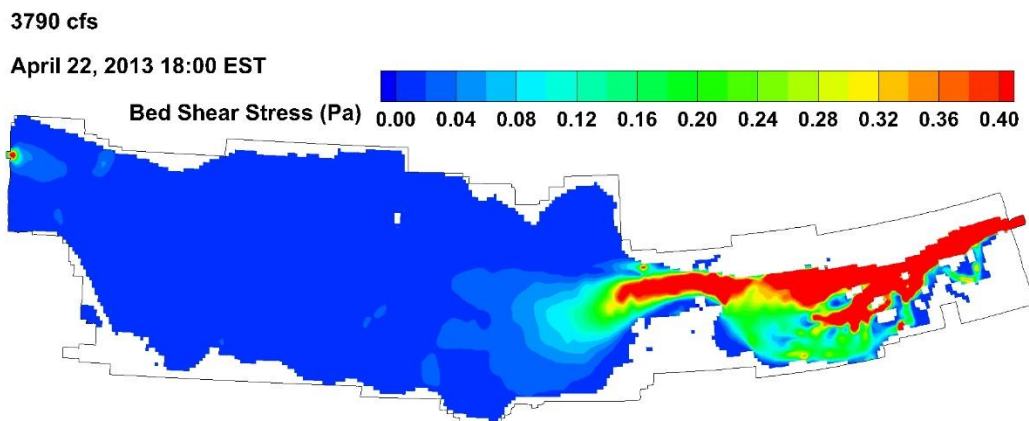


Figure 23. Bed Shear Stress Distribution at Discharge $Q = 3790$ cfs

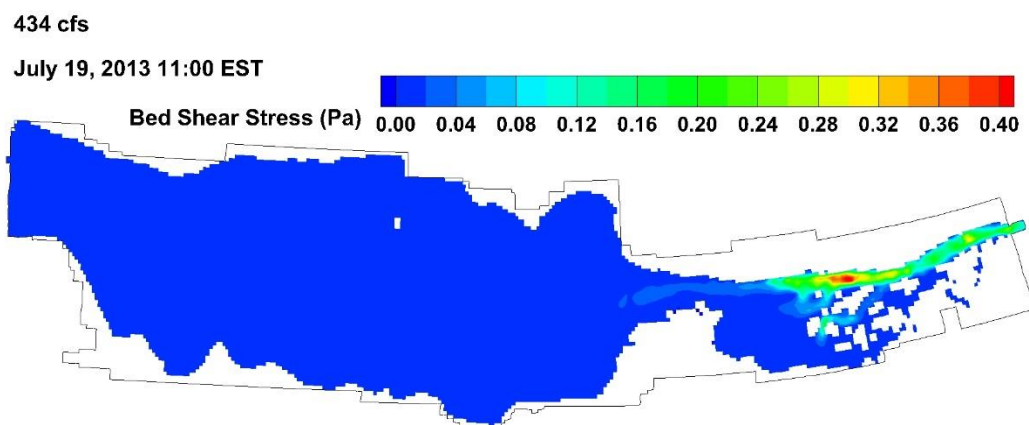


Figure 24. Bed Shear Stress Distribution at Discharge $Q = 434$ cfs

Bed shear stress distributions under high and low inflow scenarios are shown in Figure 23 and Figure 24. During low flows, the particles transported from upstream would mostly deposit in the delta. It is expected that few particles may migrate beyond the neck at the downstream end of delta. On the other hand, in high flow scenario high bed-shear stresses extend into the lake. However, Figure 23 also shows that the bed shear stress decreases dramatically once the flow passes the neck area. Obviously higher flows would more capacity to transport particles, including OPA, into the deeper areas of Morrow Lake.

3.3.3 Effect of Dam Operation

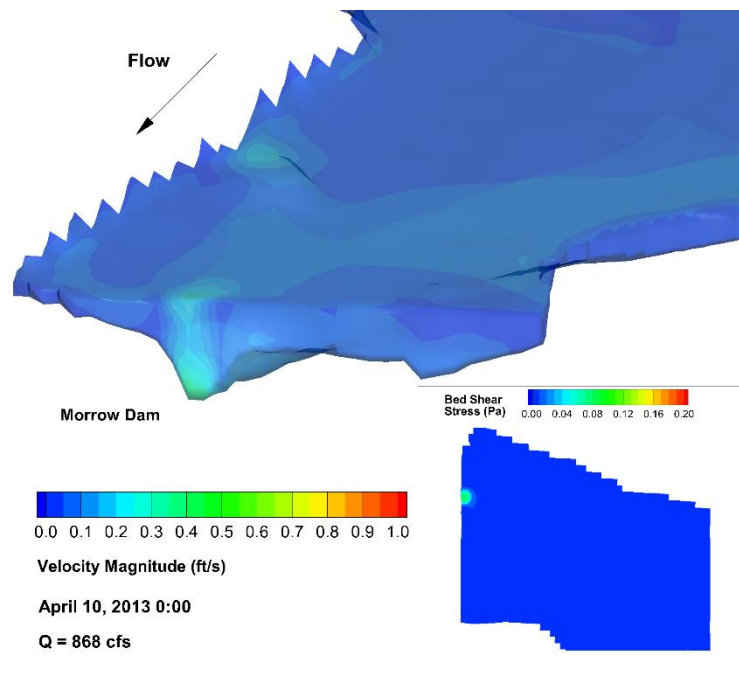


Figure 25. Velocity and Bed Shear Stress Distribution near Morrow Dam

(Q = 868 cfs with three turbines in operation)

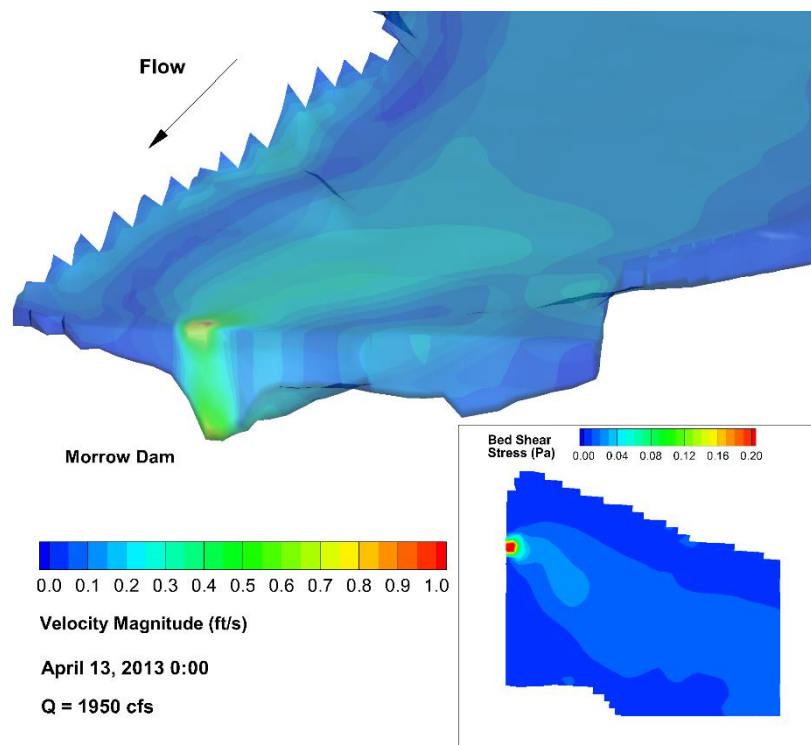


Figure 26. Velocity and Bed Shear Stress Distribution near Morrow Dam

(Q = 1950 cfs with four turbines in operation and flap gate open)

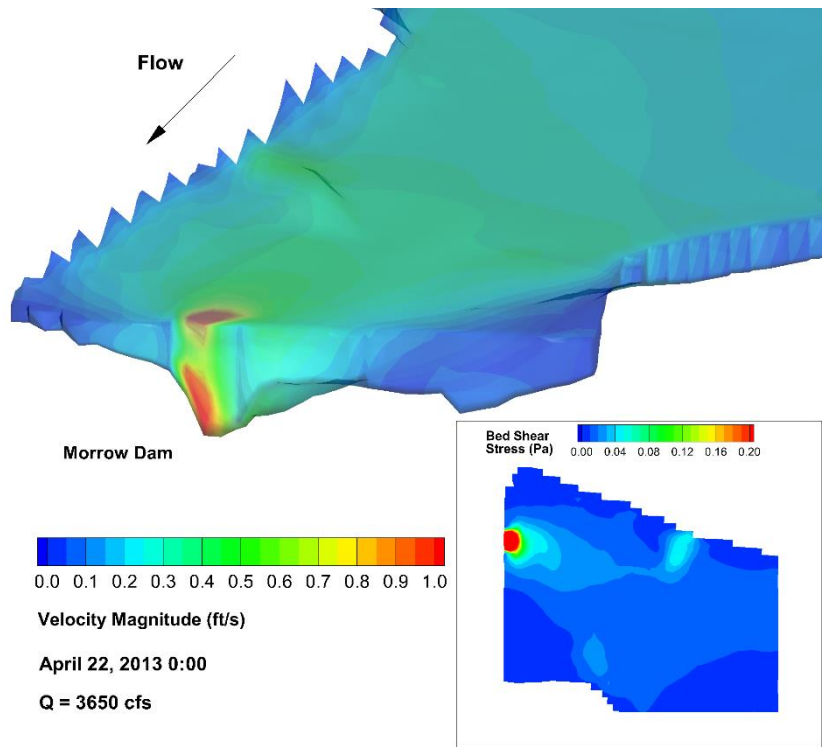
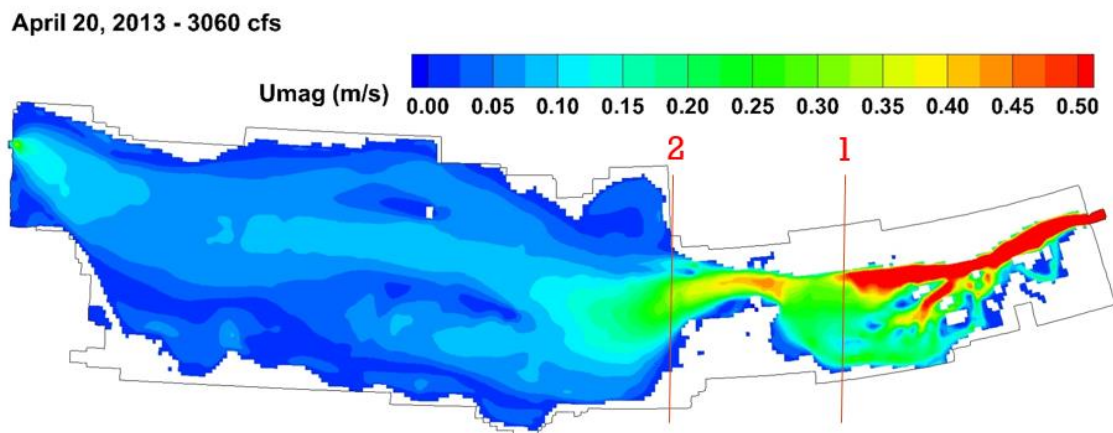


Figure 27. Velocity and Bed Shear Stress Distribution near Morrow Dam ($Q = 3650$ cfs with four turbines in operation and both flap and Tainter gates open)

Figure 25, Figure 26, and Figure 27 show the distribution of velocity magnitude and bed shear stress near the Morrow Dam with different flow discharge resulting from dam operations. The velocity and bed shear stresses increase as outflow discharge increases. However, the increase is obvious near the dam but not so obvious far away from the vicinity of the dam.

3.3.4 Sectional View of Velocity Distribution ($Q = 3060$ cfs)



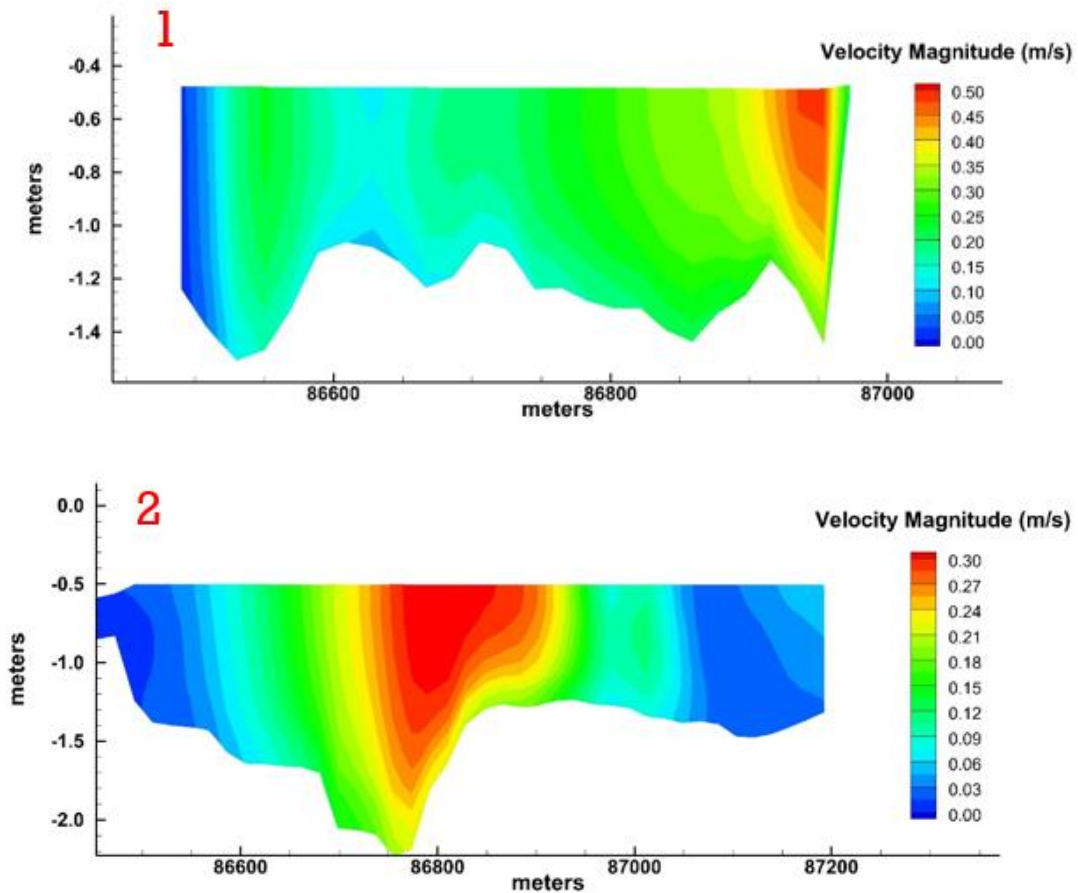


Figure 28. Plan and Sectional View of Velocity Distribution ($Q = 3060$ cfs)

Figure 28 contains a diagram of a plan view of velocity magnitude in the lake when flow discharge was 3060 cfs. Two sections were chosen to show cross-sectional views of the velocity distribution (Figure 28). The upstream section showed higher velocities in the channel along the north edge. The downstream cross section indicated water flow more to the south due to lower bed elevation in the south associated with the pre-dam channel.

3.4 OPA Tracking Model Results

The authors developed a three-dimensional Lagrangian particle tracking model which was coupled with three-dimensional EFDC hydrodynamics model. The transport of OPA contained two parts. One was transport in water; the other was interaction (including deposition and re-suspension) between the bed and water column. The transport in the water body depended on flow structure. The particle tracking model considered the advection, diffusion and settling of OPAs in the water body. A reflection boundary condition was applied to the water surface, walls, and wet-dry boundaries. For the bed

boundary, particles could deposit or be re-suspended depending on bed shear stress exerted by the flow and the specified critical bed shear stress for erosion. The Lagrangian particle tracking model allowed to specify different properties such as settling velocity and critical bed shear stress for each OPA particle. The model may not directly tell the concentration of OPA in given areas specifically. However, it can show where OPAs with certain properties would deposit and which types of OPAs are more likely able to pass through the dam under high or low flow scenarios. Quantification of OPAs concentration would be a worthwhile effort but is outside the scope of work.

3.4.1 April 2013 High Flow Scenario

Figure 29 to Figure 37 show plan views of particle locations in the April 2013 high flow scenario simulation. 8000 particles were released near the upstream inlet, which were uniformly distributed in the 8 vertical layers. The model allowed each particle to have individual properties. In this case it was assumed that all particles had the same properties. Typical OPA properties were assumed in this study. Settling velocity was specified as 1 mm/s and critical bed shear stress was assumed as 0.1 Pa. The results can be viewed by ArcGIS (for plan view) or Tecplot (for 3D view). The following figures were plotted with ArcGIS.



Figure 29. OPA Particle Locations at Time = 0 hour

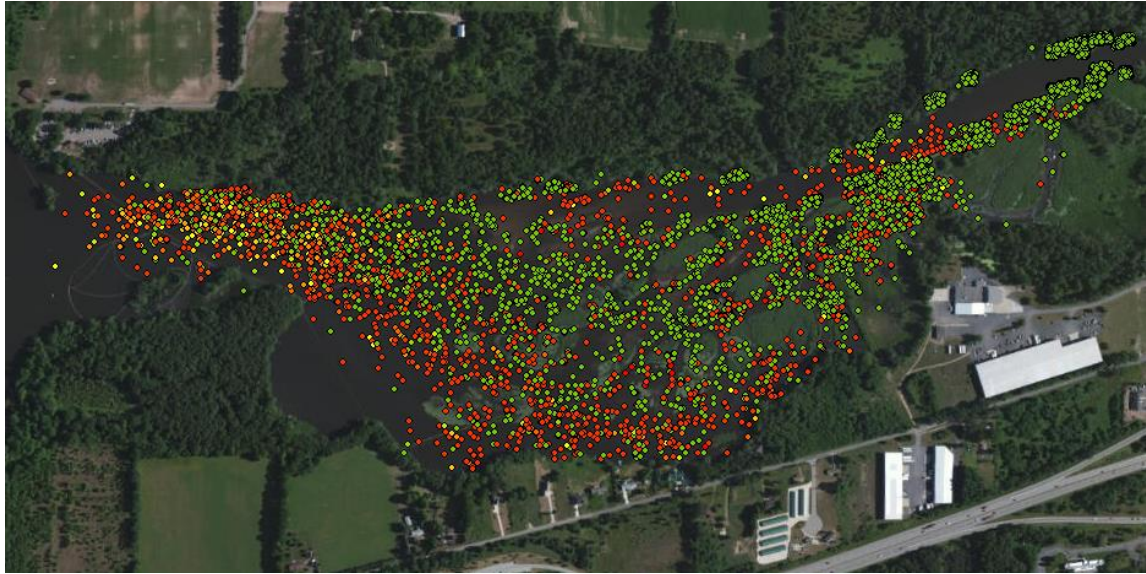


Figure 30. OPA Particle Locations at Time = 4 hour (Q = 690 cfs)

The color of particles indicates relative depth. Red dots mean particles are closer to the water surface while green ones mean they are closer to the bottom. At time = 4 hours, some particles already deposited, but many of them were still flowing downstream.

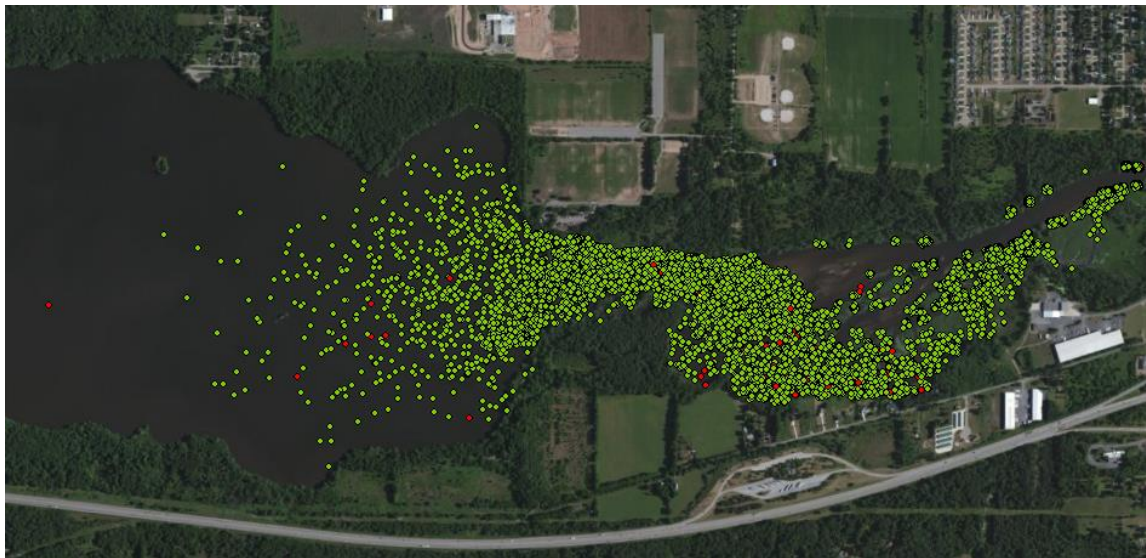


Figure 31. OPA Particle Locations at Time = 24 hour (Q = 868 cfs)

After 24 hours, simulation results indicated that most particles reached the bottom. Many particles deposited in the delta while some of them passed the delta and neck areas into the lake.

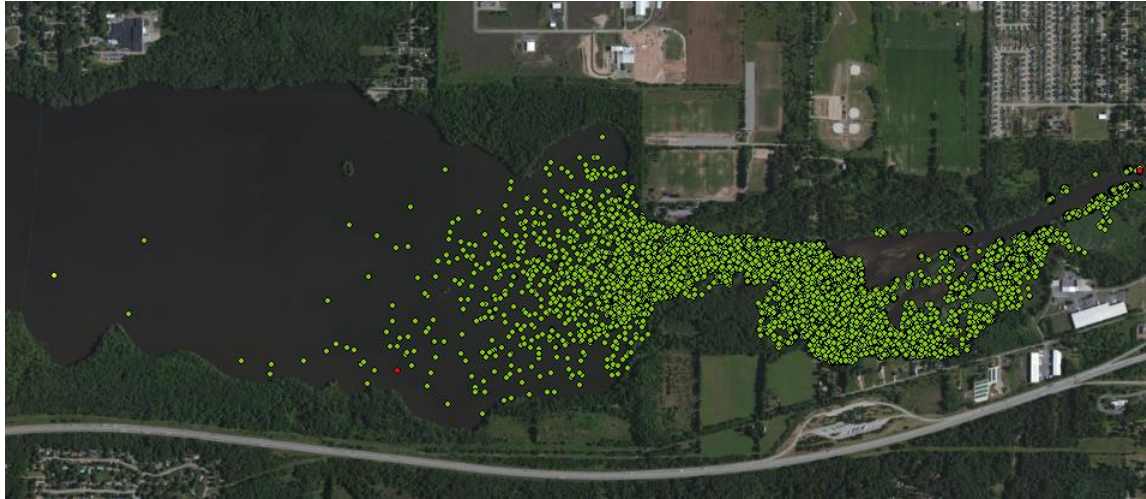


Figure 32. OPA Particle Locations at Time = 2 day (Q = 884 cfs)

After 2 days almost all particles deposited. Because the flow discharge was in a relatively low range in the first two days, if bed shear stress was less than critical bed shear stress, particles that deposited would stay until the flow intensity increased such that bed shear stresses sufficient to entrain them into the water column were achieved.

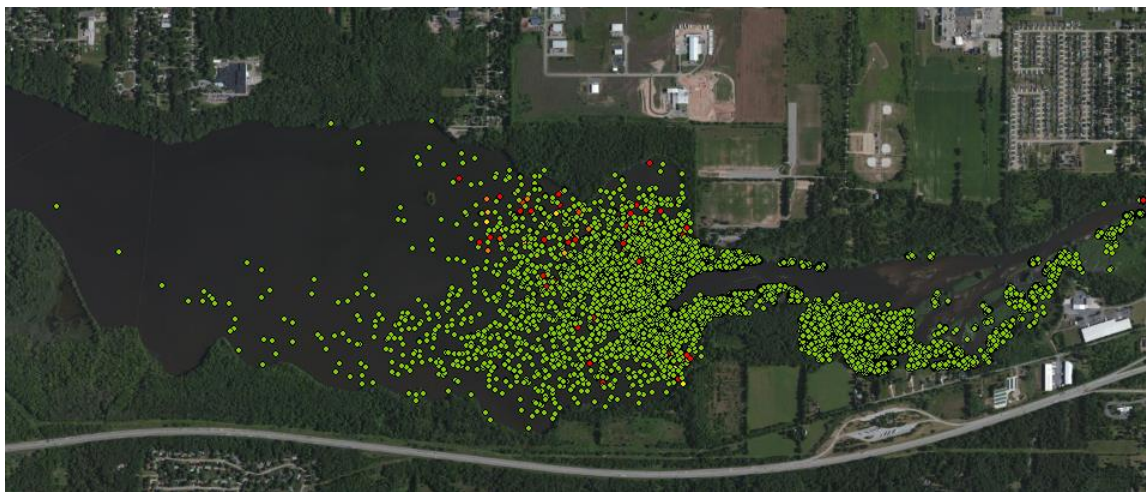


Figure 33. OPA Particle Locations at Time = 4 day (Q = 1940 cfs)

At time = 4 days, flow discharge increased to 1940 cfs. As flow increased, bed shear stresses increased and could exceed the critical bed shear stress for erosion of OPAs. OPAs were entrained and transported downstream. This phenomena was obvious in the upper part of the delta and channel portion of the neck areas.



Figure 34. OPA Particle Locations at Time = 8 day ($Q = 2440$ cfs)

Similar to Figure 33, flow discharge kept increasing so more particles were re-suspended. The change happened mainly in the delta and neck areas because bed shear stresses in the lake were still not sufficiently high to support particle resuspension. Particles entrained from the delta and neck areas all deposited in the lake.



Figure 35. OPA Particle Locations at Time = 13 day ($Q = 3660$ cfs)

After 13 days, inflow reached the maximum magnitude in this scenario. Deposition areas in the delta were much reduced. More particles were found to migrate into the lake.



Figure 36. OPA Particle Locations at Time = 15 day (Q = 3230 cfs)

After 15 days, all particles deposited and almost nothing changed from time = 15 days to time = 20 days because inflow discharge decreased. Some deposition areas were observed in the delta. Many particles were distributed in the lake but none passed the dam. However, some of them were already close to the downstream end.

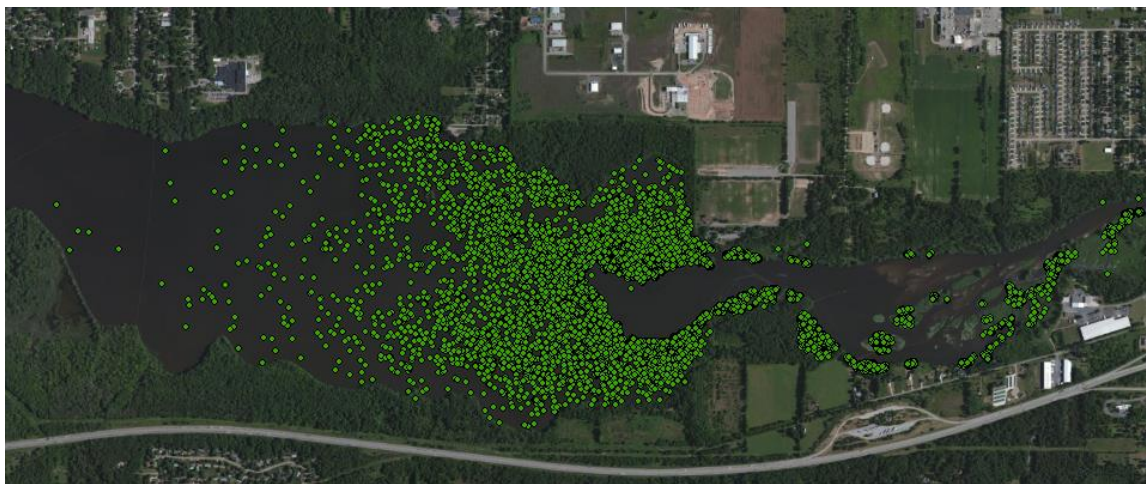


Figure 37. OPA Particle Locations at Time = 20 day (Q = 2250 cfs)

The properties of OPA remaining in the Kalamazoo River waterways were studied in related efforts by Waterman and Garcia (2015) and Hayter et al. (2015). Three different types of OPAs were characterized and their Stokes settling velocities estimated as 75.54 (Type 1), 0.23 (Type 2), and 2.78 (Type 3) mm/s, respectively (Fig. 38). The critical shear stress was assumed to be constant, 0.1 Pa, although the Lagrangian particle tracking model allows for specifying each particle with different critical shear stress as

well as other properties. The location of all particles at the end of the simulation is shown in Figure 39.

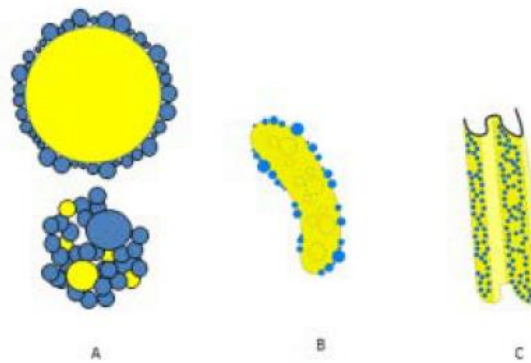


Figure 38. Types of OPA

(A) single and multiple droplet aggregate; (B) solid aggregate of large, elongated oil mass with interior particles (dashed blue circles); (C) flake aggregate of thin membranes of clay aggregates that incorporate oil and fold up. Blue color represents particles and yellow represents oil (after Fitzpatrick et al. 2015)

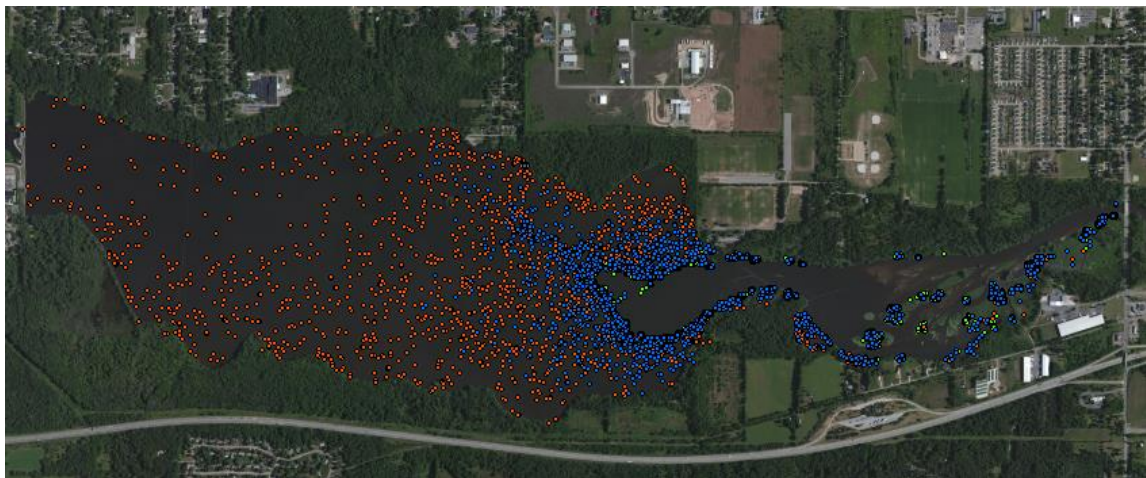


Figure 39. OPA Particle Locations at the end of simulation
(Type 1 as green; Type 2 as red; Type 3 as blue)

All type 1 and type 3 OPAs were deposited at the end of simulation; while some of type 2 OPAs might migrate through the downstream dam. It is worth mentioning that most likely different types of OPAs have different critical bed shear stress. Also, potential armoring effects were not considered which meant all particles were assumed to be on the top of the lake bed. They can be picked up by flow that provides larger bed shear stress than the critical bed shear stress for erosion.

3.4.2 July 2013 Low Flow Scenario

The same three types of OPAs as shown above were simulated for the July 9 -19, 2013 low flow scenario. 2000 particles of each type were released at once. All particles deposited in the end of the 10-day simulation. Their location is plotted in the following figures.



Figure 40. OPA Particle (Type 1) Locations at Time = 10 day (July 2013 Scenario)

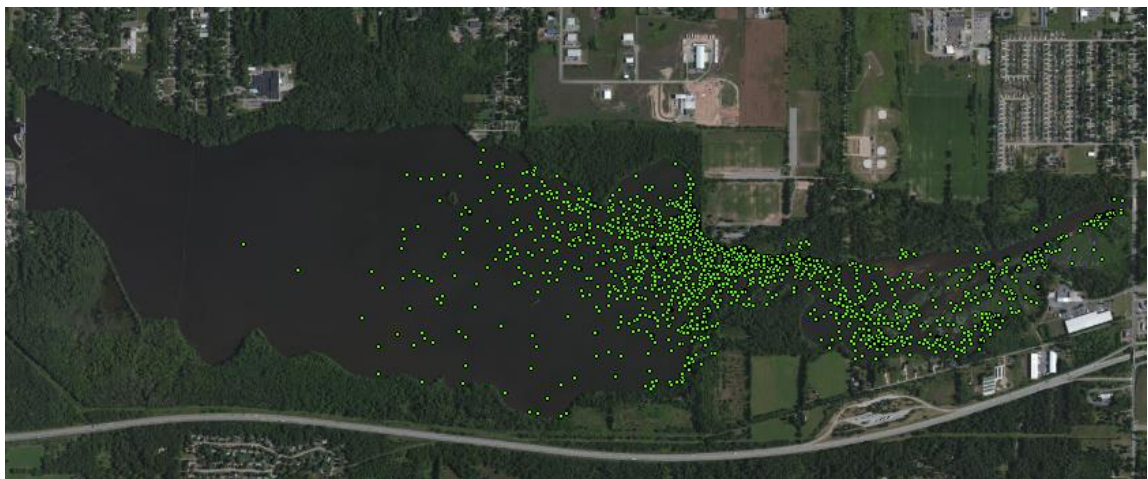


Figure 41. OPA Particle (Type 2) Locations at Time = 10 day (July 2013 Scenario)



Figure 42. OPA Particle (Type 3) Locations at Time = 10 day (July 2013 Scenario)

As shown from Figure 40 to Figure 42, more particles deposited in the delta and their transport distance was less when the settling velocity was larger. Compared to the transport of OPAs in the April 2013 high flow scenario, OPAs deposited faster and more frequently along the delta instead of migrating into the lake.

Another group of 2000 lighter particles, having a settling velocity of 0.1 mm/s and a critical shear stress of 0.01 Pa, were simulated too (see Figure 43). As expected lighter particles have more possibility of passing downstream of the dam. Some particles would deposit in low shear areas near the bank or floodplain. Most of those particles would pass through Morrow Lake under a more prolonged simulation even in such a low flow case.

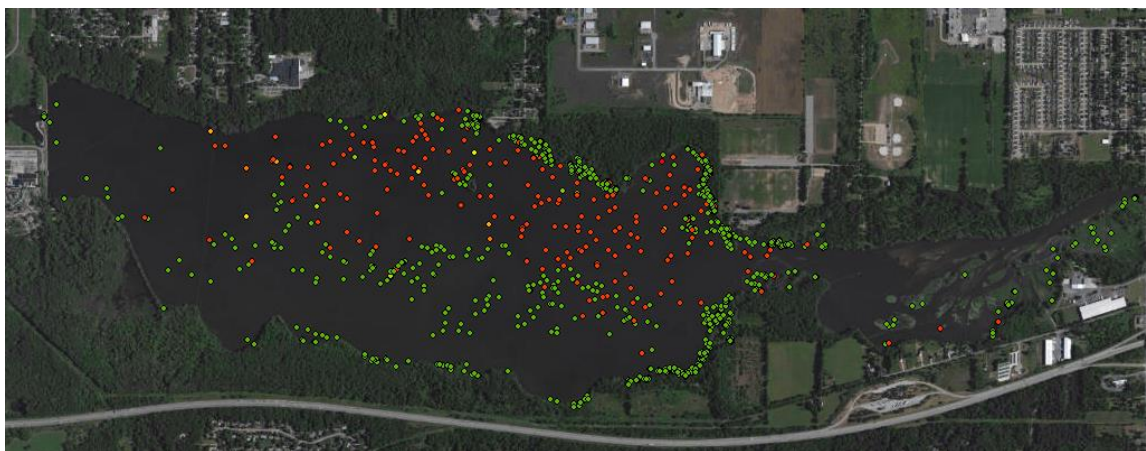


Figure 43. OPA Particle Locations at Time = 10 day (July 2013 Scenario with lighter particles)
(Red dots mean particles are close to the water surface while green ones mean they are close to the bottom.)

4. Model Applications

4.1 Containment Scenario

The developed three-dimensional hydrodynamic model EFDC was used to simulate the effects of containment on flow pattern, in particular in the Morrow Lake delta and neck areas. Containments were used to avoid oil passing downstream during dredging operations. Figure 44 shows the deployment of containments. A front view of the containment curtain in the water column is sketched in Figure 45. The bottom curtain is two feet high if the water depth is greater than four feet. Otherwise, it was assumed that the curtain height was half of the water depth. For describing the containment configurations, EFDC is able to simulate thin barriers which block the whole water depth. However, the curtain in this study only blocks the bottom layer. Also, the thin barrier option in EFDC can block U velocity (easting-direction velocity) and/or V velocity (northing-direction velocity). However, the directions of some containments were not parallel to either easting or northing direction. Therefore, the thin-barrier option was not suitable for this study. Further development of the numerical code would be required if a half-blocking curtain with diagonal direction had to be modeled. An alternative approach was proposed herein and tested.

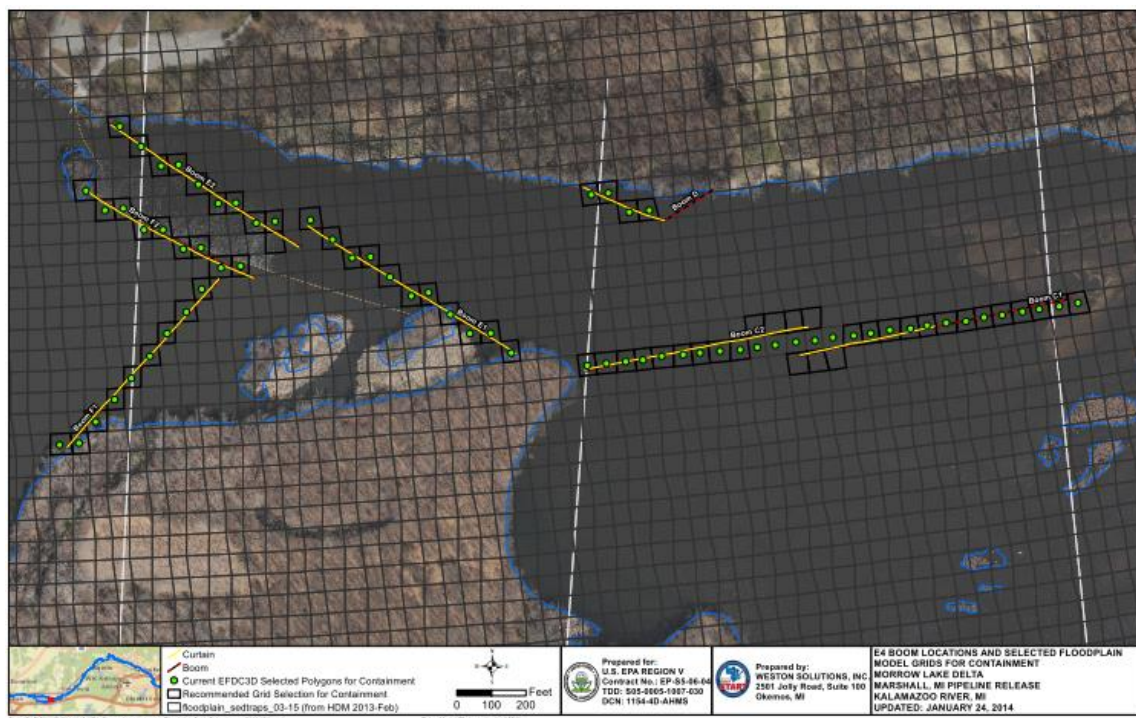


Figure 44. Location of Containment and Representative EFDC Grids

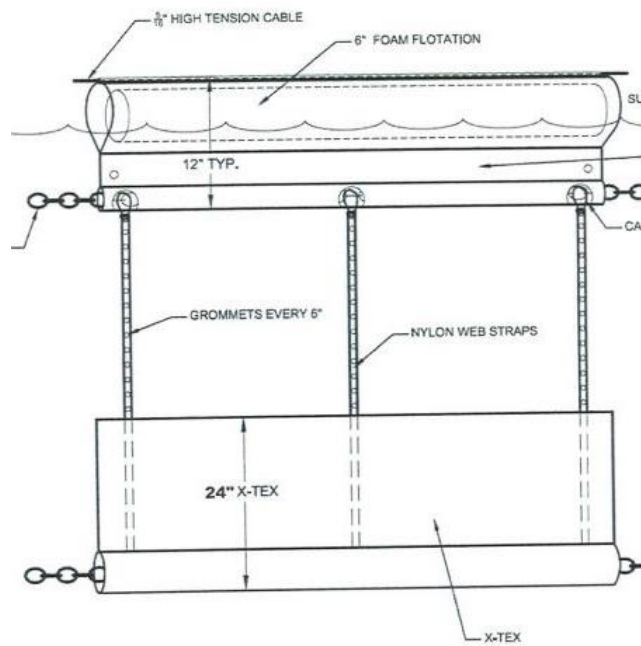


Figure 45. Curtain Vertical Detail
(Figure provided by ENBRIDGE)



Figure 46. Containment Plan View (Courtesy of Rex Johnson)

Although the curtain is very thin, it blocks flow in a certain direction (i.e. water cannot cross the curtain) locally. In order to describe the curtain in EFDC, we assumed it could affect a distance of $\Delta x/2$ on both sides of the curtain where Δx was the grid size, which was around 60 feet in the current model. For example, in Figure 47 the blue line represents the real curtain which blocks flow crossing it. It was assumed that the effect of the curtain extends some distance away from it. In this affected area, velocity in the direction perpendicular to the curtain was negligible. Therefore those vertical cells covering the curtain from the bottom can be deleted and the upper cells can still be simulated. A drawback of this approach is that it does not allow results to be obtained very close to the curtain. However, from its neighboring grid cells one can at the very least better understand any flow pattern or bed shear stress change due to the curtain.

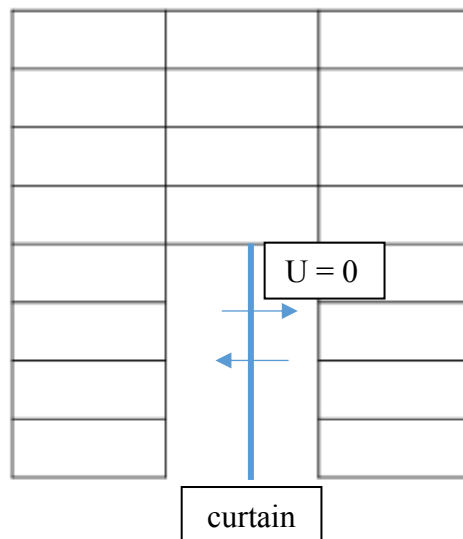


Figure 47. A Side View of Vertical Profile of EFDC Grids Representing Bottom Curtain

The curtain design was tested with a low flow of 500 cfs which corresponded to the August 27, 2012 flow when ADCP measurement data were available for comparison. Downstream water level was estimated as 775 ft although a field measurement was not made on August 27, 2012 (see Figure 48). Compared to water stage level in June and July 2012, stage level in August was probably similar since outflow discharge was similar.

ADCP measurements were performed at eight cross sections (see Figure 49). The comparison between flow discharge evaluated by ADCP and model results is summarized in Table 1.

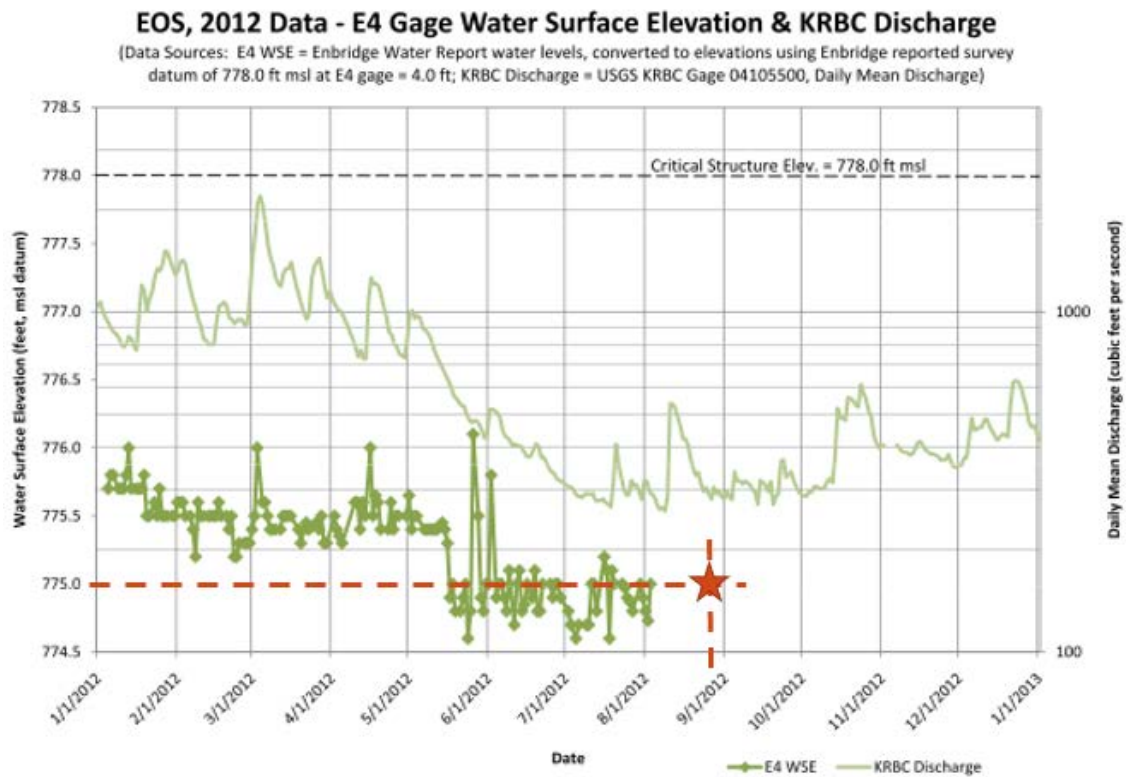


Figure 48. Data of Dam Outflow Discharge (green line) and Stage Level (scatter with green line) (Courtesy of Rex Johnson; red dash line shows the estimation of stage level for August 27, 2012)

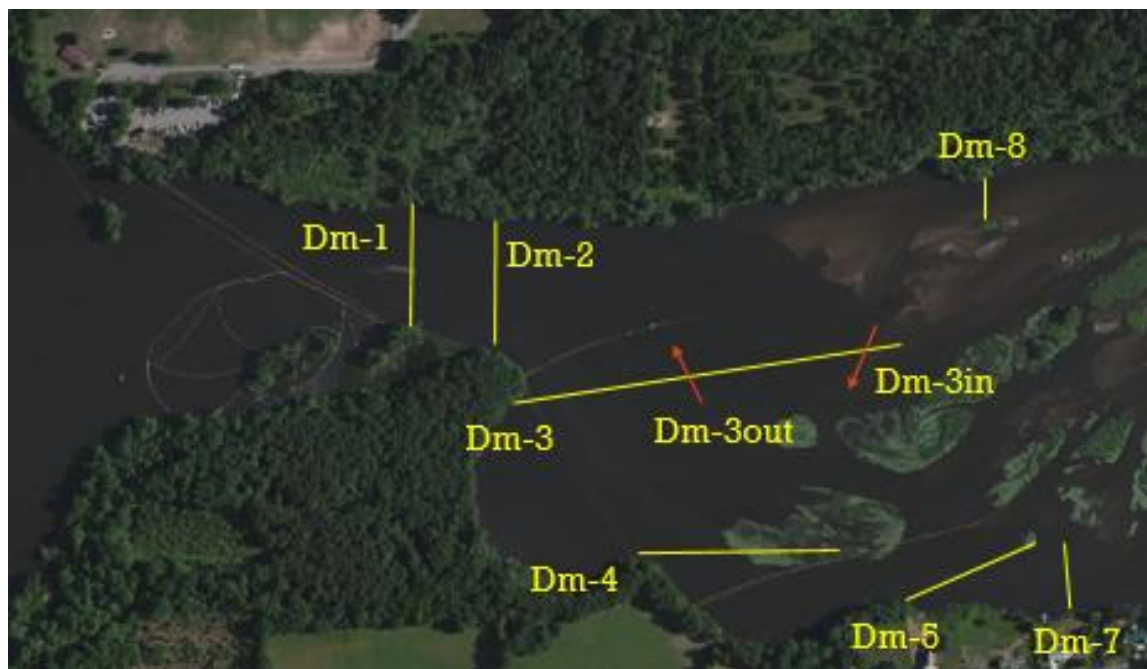


Figure 49. Cross-sections for Flow Discharge Check

Table 1. Flow Discharge Distribution (ADCP Measurement vs. Model Results)

Transect	ADCP	Model
Dm-1	502 cfs	500 cfs
Dm-2	517 cfs	500 cfs
Dm-3	189 cfs	172 cfs
Dm-3in		-12 cfs
Dm-3out		184 cfs
Dm-4	126 cfs	70 cfs
Dm-7	58 cfs	23 cfs
Dm-8	132 cfs	209 cfs

In general, the comparison shows good agreement at transect Dm-1, Dm-2, and Dm-3. However there is a relatively larger difference at Dm-4, Dm-7, and especially at Dm-8. The most likely reason is that the channel at Dm-8 is so narrow and was represented by only two grid cells in the (x, y) plane. Therefore, bathymetry and interpolation of bed elevation would highly affect the flow distribution. Similar effects by the interpolation might happen at Dm-4 and Dm-7. Possibly the estimated 500 cfs constant inflow rate and downstream stage level might also affect the model results since it is very likely that the inflow may have been different and changing in time.

The same boundary conditions were used for a simulation without containment so the difference caused by the curtains could be evaluated. The differences of velocity magnitude for with and without containment scenarios are presented in Figure 53.

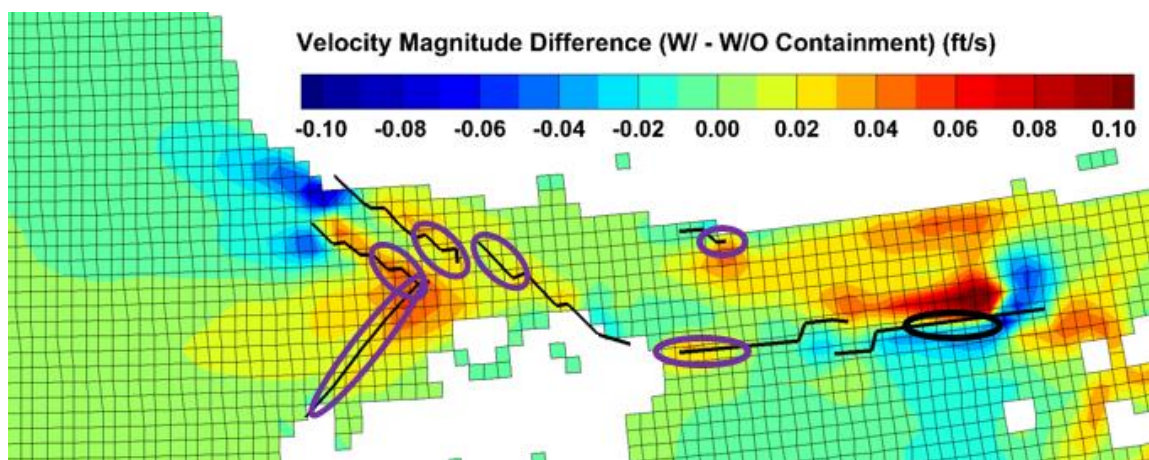


Figure 50. Deposition (black ellipse) and Erosion (purple ellipse) Areas with Velocity Difference between the scenarios with and without Containment

The comparison of model results between the scenarios with and without containment shows the effects of containment on flow distribution. Figure 50 shows the difference of velocity magnitude. It is worth mentioning that the judgment of whether the model approach is sufficient requires field measurement and experience. The ADCP measurement data was helpful, but there was no data for the non-containment scenario so it was difficult to validate the effects of containment shown in the model.

Other available data included 6 sets of bathymetric survey data on both sides of the curtains. The bathymetry survey indicated whether deposition or erosion happened on both sides of each containment. Figure 50 shows those areas with deposition as black ellipses and erosion areas with purple ellipses. Again it is worth pointing out that either deposition or erosion shown by the survey cannot simply be assumed to be directly caused by the containment curtains. Depending on the flow rate between survey periods, natural sediment deposition or erosion may have occurred regardless of the containment. However, according to model results, the existence of containment probably enhanced deposition or erosion by affecting velocity fields.

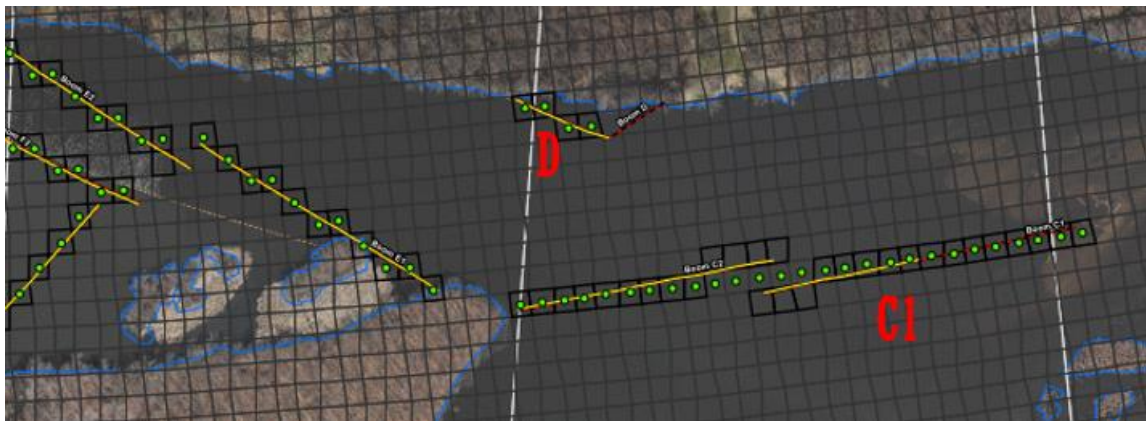


Figure 51. Location of Containment C1 and D

With the help of the numerical model, it was suggested that containment C1 and D (see Figure 51 for location) might be removed so that the effects on morphological change can be reduced and meanwhile the function of the containment system was not entirely eliminated. A set of simulations with inflow $Q = 2320$ cfs were provided. Figure 52 to Figure 54 compare distributions of bed shear stress between different simulations, i.e. original containment, no D and half C1, and no C1.

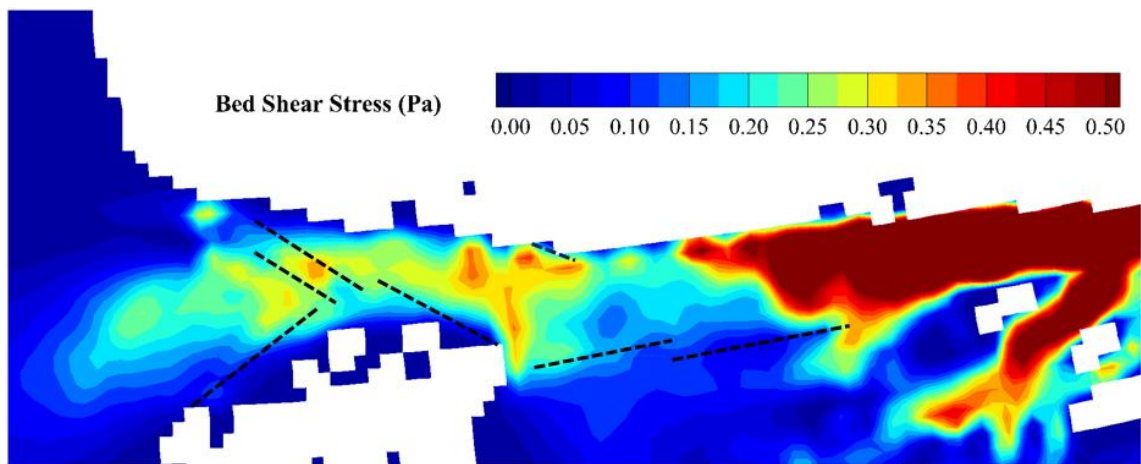


Figure 52. Distribution of Bed Shear Stress (with Original Containment Design)

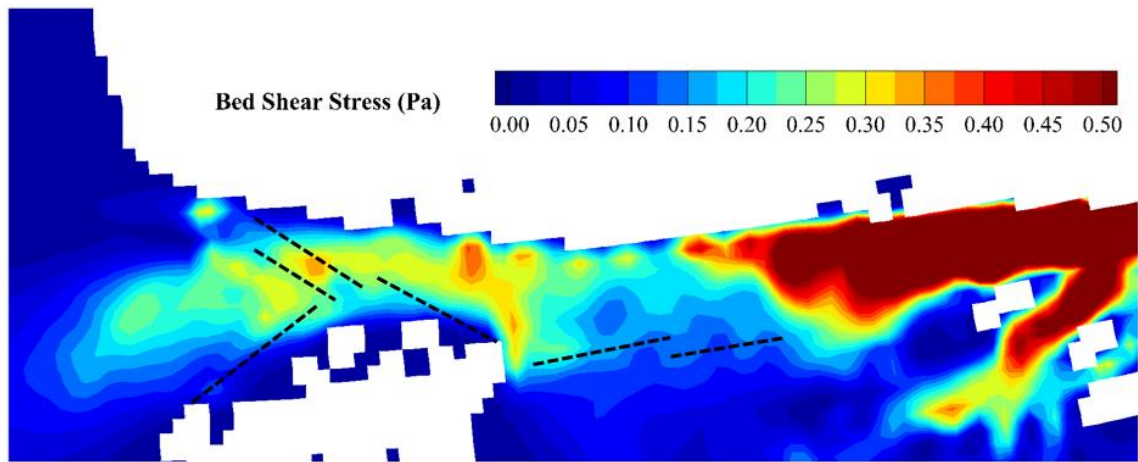


Figure 53. Distribution of Bed Shear Stress (without Containment D and Half C1)

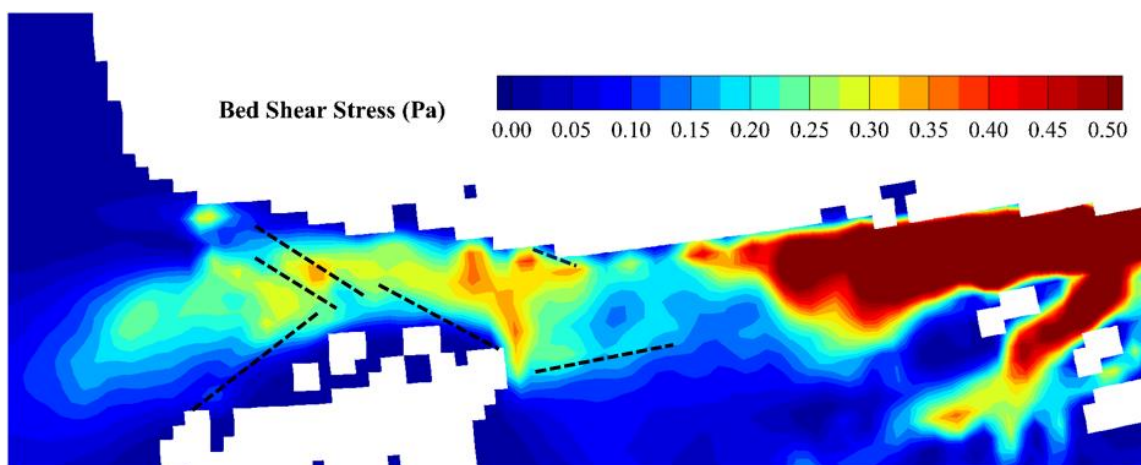


Figure 54. Distribution of Bed Shear Stress (without Containment C1)

4.2 Lake Drawdown Scenario

Another application of the developed model was to study possible drawdown scenarios of the Morrow Lake. Enbridge proposed the drawdown of the lake in order to make the excavation of the delta easier and cheaper. This model was used to evaluate how much drawdown was needed and which flow conditions were suitable for the drawdown.

According to historical flow measurement at USGS Comstock station (see Figure 6), the median daily mean flow between July 1st and October 31st is 585 cfs while that between November 1st and January 31st is 794 cfs. It was assumed that the initial lake level was 775.0 ft.

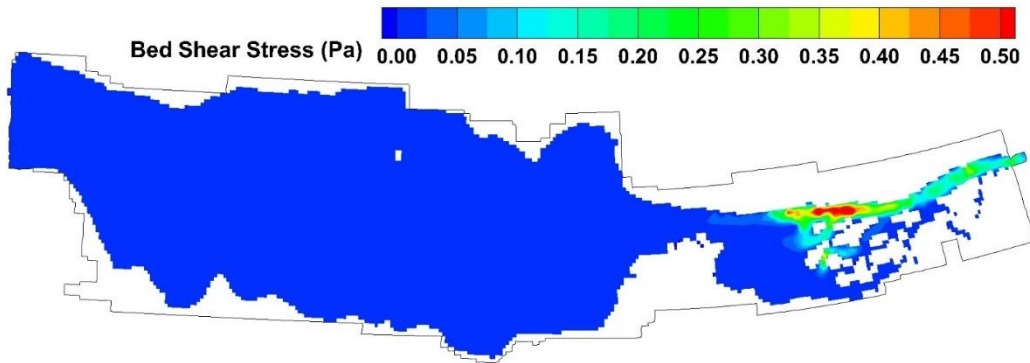


Figure 55. Distribution of Bed Shear Stress (Q = 585 cfs; DS Level = 775 ft)

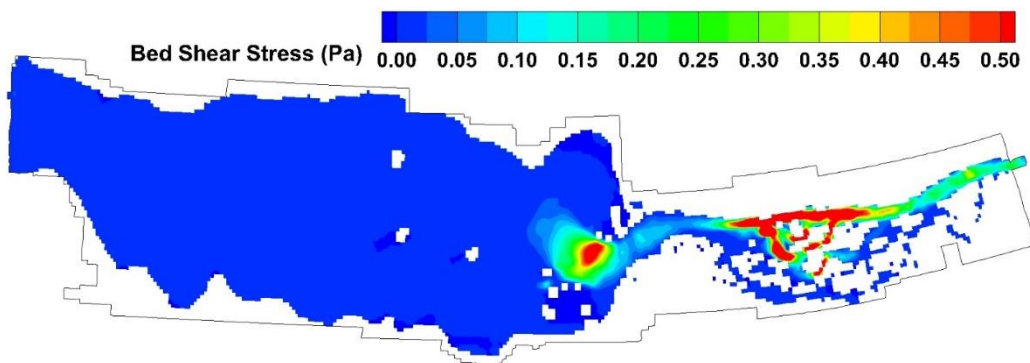


Figure 56. Distribution of Bed Shear Stress (Q = 585 cfs; DS Level = 773 ft)

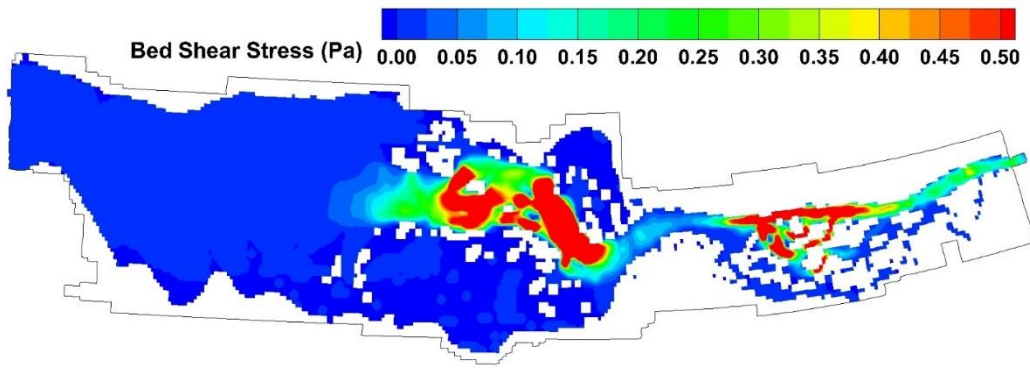


Figure 57. Distribution of Bed Shear Stress (Q = 585 cfs; DS Level = 771 ft)

When flow discharge was 585 cfs, it was found that the downstream stage of 773 ft gave similar dry areas in the delta observed for a stage of 771 ft. However, 771 ft resulted in much higher bed shear stresses in the lake. It was also noted that 773 ft would dramatically increase bed shear stresses so the risk of OPA resuspension and transport had to be considered by decision makers on site.

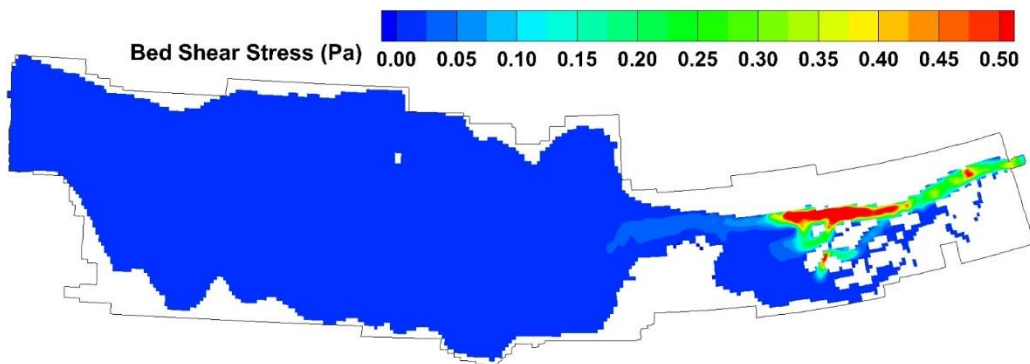


Figure 58. Distribution of Bed Shear Stress (Q = 794 cfs; DS Level = 775 ft)

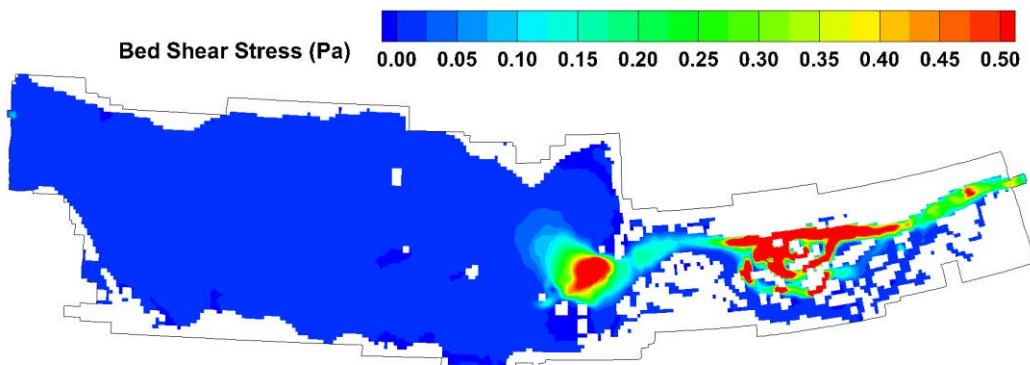


Figure 59. Distribution of Bed Shear Stress (Q = 794 cfs; DS Level = 773 ft)

When flow discharge increased to 794 cfs, drawdown of Morrow Lake would cause more substantial change to the bed shear stress distribution. The critical bed shear stress for OPA is around 0.1 Pa. Therefore, a drawdown of Morrow Lake could highly increase the possibility of passing OPA through the downstream dam.

Finally, it should be noted that the numerical model can help to compute how much outflow discharge is needed in order to decrease lake stage level with a certain rate; the bed shear stresses in this transient drawdown condition could be readily determined.

5. Summary

A three-dimensional model of Morrow Lake and its delta was built using the EFDC code to simulate the hydrodynamics. A Lagrangian particle tracking model was coupled with the hydrodynamics model to simulate the fate and transport of OPA.

The April 2013 high flow scenario and the July 2013 low flow scenario were modeled. The model was calibrated and validated using field measurement data. The transport of OPA with different particle properties was modeled for both high and low flow scenarios.

The model was applied to two cases: a containment scenario and a Morrow Lake drawdown scenario. The applied cases demonstrated the utility of the numerical model in assisting with management decisions.

The model can be improved with better knowledge of OPA properties in Kalamazoo River. Some laboratory experiments have been performed in the Ven Te Chow Hydrosystems Laboratory in order to gain a better understanding of the physics of OPAs. The authors plan on using such experimental data to test and improve the predictive capabilities of the OPA tracking model.

Acknowledgments

The authors would like to thank Faith Fitzpatrick of the USGS Wisconsin Water Science Center for coordination and help throughout the project. David Soong of the USGS Illinois Water Science Center is acknowledged for providing advice regarding the modeling and report. Rex Johnson of GRT is acknowledged for providing data and other useful information. STS Hydropower Ltd (STS) is acknowledged for providing data on lake water levels and dam operation.

Special thanks are given to U.S. Environmental Protection Agency and Enbridge Energy, L.P., contractors and collaborators involved in assessment and monitoring as well as recovery and containment at the Kalamazoo River site.

Bibliography

1. Fitzpatrick, F.A., Johnson, R., Zhu, Z., Waterman, D., McCulloch, R.D., Hayter, E.J., Garcia, M.H., Boufadel, M., Dekker, T., Hassan, J.S., Soong, D.T., Hoard, C.J. & Lee, K. Integrated modeling approach for fate and transport of submerged oil and oil-particle aggregates in a freshwater riverine environment. Proceedings of the 10th Federal Interagency Sedimentation Conference, Reno, NV (2015).
2. Hamrick, J. A three-dimensional environmental fluid dynamics computer code: Theoretical and computational aspects. Technical Report 317 in Applied Marine Science and Ocean Engineering, Virginia Institute of Marine Science, School of Marine Science (1992).
3. Hayter, E., McCulloch, R., Redder, T., Boufadel, M., Johnson, R. & Fitzpatrick, F. Modeling the Transport of Oil Particle Aggregates and Mixed Sediment in Surface Waters. *Technical Report*, US Army Corps of Engineers (2015).
4. Reneau, P. C., Soong, D. T., Hoard, C. J. & Fitzpatrick, F. A. Hydrodynamic Assessment Data Associated with the July 2010 Line 6B Spill into the Kalamazoo River, Michigan, 2012-14 (2015).
5. Sinha, S., Liu, X. & García, M. H. Three-dimensional hydrodynamics modeling of the Chicago River, Illinois. *Environmental Fluid Mechanics*. (2012), 12:471–494.
6. Sinha, S., Liu, X. & Garcia, M. H. A Three-Dimensional Water Quality Model of Chicago Area Waterway System (CAWS). *Environ. Model. Assess.* (2013).
7. Waterman, D. & Garcia, M. H. Laboratory Tests of Oil-Particle Interactions in a Freshwater Riverine Environment with Cold Lake Blend Weathered Bitumen.

Technical Report, Ven Te Chow Hydrosystems Laboratory, University of Illinois at Urbana-Champaign (2014).

8. Waterman, D., Fytanidis, D. & Garcia, M. H. Kalamazoo River In Situ Flume Bed Erosion Study Final Report. *Technical Report*, Ven Te Chow Hydrosystems Laboratory, University of Illinois at Urbana-Champaign (2015).